NASA CR-141865
ERIM 109600-17-F

Final Report

YIELD PREDICTION BY ANALYSIS OF MULTISPECTRAL SCANNER DATA

JOHN E. COLWELL AND GWYNN H. SUITS
Infrared and Optics Division

MAY 1975

(NASA-CR-141865) YIELD PREDICTION BY ANALYSIS OF MULTISPECTRAL SCANNER DATA Final Report, 15 May 1974 - 14 Mar. 1975 (Environmental Research Inst. of Michigan) 82 p HC $4.75 CSCL 02C G3/43
N75-26476
Unclas 26649

Prepared for
NATIONAL AERONAUTICS AND SPACE ADMINISTRATION
Johnson Space Center
Earth Observations Division
Houston, Texas 77058

Contract No. NAS9-14123, Task IX
Technical Monitor: Dr. A. Potter/TF3

ENVIRONMENTAL
RESEARCH INSTITUTE OF MICHIGAN
FORMERLY WILLOW RUN LABORATORIES THE UNIVERSITY OF MICHIGAN
BOX 618 • ANN ARBOR • MICHIGAN 48107

NOTICES

Sponsorship. The work reported herein was conducted by the Environment Research Institute of Michigan for the National Aeronautics and Space Administration, Earth Observations Division. Lyndon B. Johnson Space Center, Houston, under contract NAS9-14123. Dr. Andrew E. Potter/TF3 is Technical Monitor for NASA. Contracts and grants to the Institute for the support of sponsored research are administered through the Office of Contracts Administration.

TECHNICAL REPORT STANDARD TITLE PAGE

1. Report No. NASA-CR- ERIM 109600-17-F	2. Government Accession No.	3. Recipient's Catalog No.
4. Title and Subtitle YIELD PREDICTION BY ANALYSIS OF MULTISPECTRAL SCANNER DATA		5. Report Date May 1975
		6. Performing Organization Code
7. Author(s) John E. Colwell and Gwynn H. Suits		8. Performing Organization Report No. 109600-17-F
9. Performing Organization Name and Address Environmental Research Institute of Michigan Infrared and Optics Division P.O. Box 618 Ann Arbor, Michigan		10. Work Unit No. Task IX
		11. Contract or Grant No. NAS9-14123
12. Sponsoring Agency Name and Address National Aeronautics and Space Administration Johnson Space Center Houston, Texas 77058		13. Type of Report and Period Covered Final Technical Report 15 May 1974 to 14 Mar 1975.
		14. Sponsoring Agency Code

15. Supplementary Notes

The work was performed for the Earth Observations Division. Dr. Andrew Potter was the Technical Monitor.

16. Abstract

A preliminary model describing the growth and grain yield of wheat has been developed. The modeled growth characteristics of the wheat crop have been used to compute wheat canopy reflectance using a model of vegetation canopy reflectance. The modeled reflectance characteristics have been compared with the corresponding growth characteristics and grain yield in order to infer their relationships. It appears that periodic wheat canopy reflectance characteristics potentially derivable from earth satellites will be useful in forecasting wheat grain yield.

17. Key Words Remote Sensing Yield Prediction Growth Model	18. Distribution Statement Initial Distribution is listed at the end of this document.

19. Security Classif. (of this report)	20. Security Classif. (of this page)	21. No. of Pages	22. Price
UNCLASSIFIED	UNCLASSIFIED	82	

CONTENTS

	Page
PREFACE	3
LIST OF FIGURES	4
LIST OF TABLES	5
ABSTRACT	6
1. SUMMARY	7
2. INTRODUCTION	8
2.1 BACKGROUND	9
2.2 PURPOSE OF THE ERIM GROWTH MODEL	11
3. GROWTH MODEL DESCRIPTION	15
3.1 PHOTOSYNTHESIS	16
3.2 TRANSPIRATION	21
3.3 PRECIPITATION AND SOIL MOISTURE	23
3.4 PLANT RESPONSE	25
3.5 ENVIRONMENTAL FACTORS	26
4. GROWTH MODEL RESULTS	30
5. WHEAT REFLECTANCE MODELING	35
6. CONCLUSIONS	41
7. RECOMMENDATIONS	42
APPENDIX I Effect of Soil Reflectance Variability	43
APPENDIX II Yield Transformation	62
APPENDIX III Rules for Assigning Total Area to Component Projected Areas	63
APPENDIX IV Detailed Performance of the Growth Model	66
GLOSSARY	70
REFERENCES	71
DISTRIBUTION LIST	74

PREFACE

This final report summarizes a program of research in modeling the vegetative growth, yield, and reflectance of wheat. The research was carried out for NASA's Lyndon B. Johnson Space Center, Houston, Texas, by the Environmental Research Institute of Michigan (ERIM). The basic objective of this program was to develop remote sensing as a practical tool for obtaining information to improve the accuracy and timeliness of wheat yield forecasts.

The research covered in this report was performed under Contract NAS9-14123 and covers the period from 15 May 1974 through 14 March 1975. Dr. Andrew Potter has been the Technical Monitor for NASA, and Dr. Tom Barnett has been the Task Monitor.

Work on this contract is performed in the Infrared and Optics Division under the direction of Mr. Richard R. Legault. Dr. Jon D. Erickson, Head of the Information Systems and Analysis Department, is the project director for this contract, and Mr. Richard F. Nalepka, Head of the Multispectral Analysis Section, is the Principal Investigator.

The authors wish to acknowledge the assistance provided by Mr. R.R. Legault, particularly in making ERIM Internal Research and Development funds available to augment this work. We also wish to acknowledge the assistance of personnel of the Michigan State University Agricultural Experiment Station for providing information concerning the physiology of wheat.

LIST OF FIGURES

1a.	The Relationship Between ERIM Growth Model, Vegetation Reflectance Model, and Yield Model.	13
1.	Schematic Diagram of the Logical Structure of the ERIM Growth Model.	14
2.	Orthogonal Projections Making Idealized Biological Components.	18
3.	Schematic Diagram of Radiation Driving Photosynthetic Process in Canopy	19
4.	Schematic Flow Diagram For Photosynthesis Proposed by Lommen Et Al. For Unit Area of Leaf	20
5.	XYLEM System.	22
6.	Flow Chart for Precipitation and Soil Moisture.	24
7.	Seasonal Green PLAI and Yield Outputs of Growth Model	29
8.	Relationship Between Projected Leaf Area Duration (PLAD) and Yield For Four Preliminary Growth Model Results	31
9.	Soil Moisture and Green PLAI For Two Weather Sequences. . . .	34
10.	Reflectance of Wheat Canopy For Day 155, Weather Sequency 1960	36
11.	Wheat Canopy Reflectance in Green, Red, and IR Spectral Regions During Growing Season For Weather Sequence 1960 . . .	38
12.	Wheat Canopy Reflectance in Green, Red, and IR Spectral Regions During Growing Season for Weather Sequence 1961 . . .	39
13.	Wheat Canopy IR/Red Reflectance Ratios During Growing Season For Weather Sequence 1960 and 1961	40
Ia.	Bidirectional Reflectance of Simulated Canopies With Light Soil	46
Ib.	Bidirectional Reflectance of Simulated Canopies With Dark Soil	47
IVa.	Hourly Values of Transpiration For Three Days In the Growing Season.	67
IVb.	Hourly Values of Net Photosynthesis for Three Days in the Growing Season.	68

LIST OF TABLES

I-a. Horizontal P.L.A.I. vs. $(1-e^{-H})$ 44

I-b. Hemispherical Reflectance and Transmittance Values Used in Modeling For Vegetation Cover 45

I-c. Variability of Vegetation Canopy Spectral Reflectance Due To Variable Soil Reflectance as A Function of Percent Vegetation Cover and P.L.A.I. 48

I-d. Relative Values of Hemispherical Reflectance and Transmittance For Components of Experimental Oats Vegetation Canopies 49

I-e. Effects of Soil Reflectance On Oats Canopy Reflectance as a Function Of Percent Vegetation Cover 49

I-f. Simulated Wheat Canopy Reflectance For Light And Dark Soil as a Function of Solar Zenith Angle, θ 52

I-g. Difference in Spectral Reflectance of Simulated Wheat Canopies With Light Soil and With Dark Soil as a Function of Solar Zenith Angle, θ 52

I-h. Simulated Sugarbeets and Corn Canopy Reflectance For Light Soil and Dark Soil as a Function of Soil Zenith Angle, θ . . . 54

I-i. Difference In Reflectance Between Simulated Crop Types For Light and Dark Soil as A Function of Solar Zenith Angle, θ. . . 55

I-j. Variability in Soil Reflectance For Wet Soils and For Dry Soils 59

I-k. Variability in Soil Reflectance For a Particular General Soil Class (16 soils). 59

I-1 Variability in Soil Reflectance for All Soils in Both the Wet and Dry State 60

ABSTRACT

A preliminary model describing the growth and grain yield of wheat has been developed. The modeled growth characteristics of the wheat crop have been used to compute wheat canopy reflectance using a model of vegetation canopy reflectance. The modeled reflectance characteristics have been compared with the corresponding growth characteristics and grain yield in order to infer their relationships. It appears that periodic wheat canopy reflectance characteristics potentially derivable from earth satellites will be useful in forecasting wheat grain yield.

1

SUMMARY

In an effort to maximize the utility of earth satellite data, we have investigated the possibility of using such data to forecast the grain yield of wheat. Thusfar, the investigation has been based on theoretical models, rather than empirical data.

A preliminary model describing the growth and grain yield of wheat has been developed. The model is constrained by genetically related parameters through known or inferred physiologic processes. The vegetative growth and grain yield are affected by environmental conditions such as soil type, soil moisture, climate (radiation, temperature, relative humidity, precipitation), and weather sequence for a particular climate. Implementation of the growth model for a variety of climates indicates that it performs qualitatively in a reasonable way.

The modeled growth characteristics of the wheat crop are used to compute wheat canopy reflectance using a previously developed and field-tested model of vegetation canopy reflectance. The resultant sequential reflectance characteristics of a particular crop are then compared with the corresponding growth characteristics and grain yield to infer their relationships. Preliminary analysis of these results suggests that the sequential reflectance characteristics of the crop are indicative of certain plant characteristics which are highly correlated with wheat grain yield. It appears, therefore, that it may be possible to forecast wheat grain yield by appropriate analysis of periodic wheat canopy reflectance data such as is being collected by LANDSAT.

Many factors affect vegetation canopy bidirectional spectral reflectance, and hence affect the interpretation of what the spectral reflectance "means" in terms related to yield. Some real world problems in this regard, and possible solutions to those problems, are discussed in Appendix I.

2
INTRODUCTION

The objective of the research described in this report is to determine the optimum way of utilizing periodic remotely sensed data for forecasting the grain yield of wheat grown under common as well as extreme environmental conditions. In order to do this it was necessary to develop a model of the growth and grain yield of wheat which would describe those characteristics of wheat that are necessary for the simulation of the reflectance of the crop. The model which we have developed to describe the physical growth and production of grain of wheat will be called the ERIM Growth Model. Since the model computes wheat grain production, it could technically be called a yield model. However, this Growth Model is not a yield model in the traditional agricultural-meteorological sense in that it is not an algorithm for calculating grain yield through a series of meteorological or other variables by means of a regression equation.

Certain outputs of the ERIM Growth Model are used as inputs to the ERIM Vegetation Reflectance Model[1]. These inputs include projected leaf area index and canopy structure. This information, together with appropriate ancillary data, makes it possible to simulate the bidirectional spectral reflectance during the growth and development of wheat.

The calculated reflectances from the Vegetation Reflectance Model are compared with the yield output of the Growth Model. An analysis of these two model results could lead to a yield model which will describe the optimum way in which wheat yield can be inferred from sequential bidirectional spectral reflectance. The development of the Growth Model, and the resulting relationships between wheat canopy growth, yield, and sequential spectral reflectance measurements are described in this report.

---

[1] Suits, G.H., 1972, "The Calculation of the Directional Reflectance of a Vegetative Canopy", Remote Sensing of Environment, Vol. 2, pp. 117-125.

2.1 BACKGROUND

Traditionally, yield models, especially those for estimating economic yield of agricultural crops, have been regression equations of the form

$$\text{Yield} = a + b\,X^n + c\,Y^m \ldots,$$

where various meteorological parameters, generally those that were routinely available from weather stations. Among the numerous yield models that have been developed are those by Thomson [2] and Baier [3].

Yield models have generally been developed statistically from a large empirical data base of yield and associated meteorological parameters. The lack of detailed physiologically-based causative factors in models developed in this way has resulted in their performance having a tendency towards the following characteristics: (1) they tend to work well in "normal" years but not as well in abnormal years, precisely those years for which accurate estimates of yield are most important; and (2) they may not perform well in geographic/climatic regions other than the region for which they were developed.

Growth models generally are those which predict the development of a vegetation canopy, especially the amount of photosynthetic material produced. A number of growth models have been developed and are continuing to be developed. These include models of individual leaves e.g., [4]; [5], and models of entire

[2] Thompson, L.M., 1969, "Weather and Technology in the Production of Wheat in the United States", Journal of Soil & Water Conservation, V 24 #6, Proceedings of the IBP/PP Technical Meeting. Trebon. Published by Centre for Agricultural Publishing & Documentation, Wageningen, The Netherlands.

[3] Baier, W., 1973, "Crop-Weather Analysis Model: Review & Model Development" Journal of Applied Meteorology, V. 12 #6.

[4] Chartier, Ph. 1970. "A Model of CO_2 Assimilation in the Leaf", In Prediction and Measurement of Photosynthetic Productivity. Proceedings of the IBP/PP Technical Meeting. Trebon. Published by Centre for Agricultural Publishing & Documentation, Wageningen, The Netherlands.

[5] Lommen, P.W., C.R. Schwintzer, C.S. Yocum, and D.M. Gates, 1971. "A Model Describing Photosynthesis in Terms of Gas Diffusion and Enzyme Kinetics", Planta (Berl.) 98, 195-220.

vegetation canopies e.g.,([6] [7] [8] [9] [10] [11] [12] [13] [14])

Growth models tend to have more physiological validity associated with them than do yield models. Most growth models have been developed as engineering aids for building better (more productive) plants, and for determining better ways to grow plants [15]. In addition, growth models may have biological yield (total biomass) as their output, rather than economic yield (useful biomass) (Van Keulen, personal communication). Growth models also generally do not provide the necessary output to relate yield with a time sequence of reflectance measurements, which is our objective.

---

[6] Ross, J. 1970. "Mathematical Models of Photosynthesis in a Plant Stand", In Prediction and Measurement of Photosynthetic Productivity. Proceedings of the IBP/PP Technical Meeting. Trebon. Published by Centre for Agricultural Publishing and Documentation. Wageningen, The Netherlands.

[7] Van Keulen, H., and W. Louwerse, 1973, "Simulation Models for Plant Production", W.M.O., Symposium on Agrometeorology of the Wheat Crop", Braunschweig, Germany.

[8] Tooming, H., 1970, "Mathematical Description of Net Photosynthesis and Adaptation Processes in the Photosynthetic appartus of Plant Communities", In Prediction & Measurement of Photosynthetic Productivity.

[9] Monsi, M., 1968, "Mathematical Models of Plant Communities", Functioning of Terrestrial Ecosystems at the Primary Production Level, Proc. Copenhagen Symposium. UNESCO pp. 131-144.

[10] Duncan, W.G., Loumis, R.S., Williams, W.A., & R. Hanau, 1967. "A Model for Simulating Photosynthesis in Plant Communities", Hilgardia: 38, pp. 181-205.

[11] Haun, J.R., 1973, "Evaluation of Wheat Development Relative to Environment From Quantitative Morphological Data", Symposium on Agrometeorology of the Wheat Crop. World Meteorological Organization. Braunschweig, Germany

[12] de Wit, C.T., R. Brouwer, and F.W.T. Penning de Vries, 1971, "A Dynamic Model of Plant Growth", in Potential Crop Production, Edited by P.F. Waring and J.P. Cooper, Heinemann Education Book Ltd., London.

[13] Lupton, F.G.H., 1972. "Further Experiments on photosynthesis and Translocation in Wheat", Ann. Appl. Biol. 71:69-79.

[14] Miles, G.E., R.J. Bula, D.A. Holt, M.M. Shcreiber, and R.M. Peart, 1973, "Simulation of Alfalfa Growth", American Society of Agricultural Engineers, Paper No. 73-4547, St. Joseph, Michigan.

[15] Waggoner, P.E., 1970, "Consultation on How Models are Made, How They are Tested and What They Tell Us of Experiments to be Done", In Prediction and Measurement of Photosynthetic Productivity. Proceedings of the IBP/PP Technical Meeting, Trebon, Published by Centre for Agricultural Publishing and Documentation, Wageningen, The Netherlands.

2.2 PURPOSE OF THE ERIM GROWTH MODEL

Our goal is to derive a reliable and accurate functional relation between a time series of signals caused by reflection, and the expected yield of grain using a growth model as the best available means for such a derivation. The purpose of ERIM developing a growth model incorporating physiological and environmental detail is not to advance the state of knowledge in plant physiology, growth modeling, or "yield modeling" in the traditional sense, but rather is to supply the necessary means to an end, which is to interpret correctly the significance of periodically, remotely sensed field reflectances with regard to probable field conditions and, hence, the probable yield to be expected. Consequently, the form and contents of the ERIM Growth Model are governed entirely to serve that yield forecasting end.

It is important to bear in mind the nature of that end objective. We are attempting to interpret signals of reflected daylight where the mechanism of reflection is intimately related to the mechanism of photosynthetic production.

There is no large reservoir of reflectance data which can presently be correlated with field development and eventual yield. Thus, the interpretation of the remote sensing data collected from space must be correlated with field condition and eventual yield by way of a qualitatively realistic Growth Model and its predicted reflectances. In this way, the ERIM Growth Model, itself, is not used to predict yield directly, but rather it is a means by which meaningful implications between reflectance measurements and yield can be learned. The Growth Model need not be quantitatively accurate as long as it responds correctly in a qualitative manner. The ERIM Growth Model and associated Reflectance Model are the next best substitutes for a very large historical data bank from which a yield model depending upon periodic reflectance values may be derived. In addition, the ERIM Growth Model can potentially be used to infer important environmental parameters that may ultimately be included in a yield model, if that proves to be necessary in order to improve the performance of a yield model which uses only data on periodic reflectance values.

We know from previous work e.g., [16] that it is frequently possible to make good estimates of vegetation development and condition of small grains by use of reflectance data. Other work e.g., [17] has shown good relationships between various aspects of vegetation development and wheat grain yield. It is expected that information on vegetative development will be particularly useful since field condition is likely to be indicative of many environmental parameters and cultural practices which affect wheat grain yield. Accordingly, we have chosen to try to infer wheat grain yield from certain aspects of vegetation development and condition which are detectable by reflectance data. We will use the Growth Model to determine which aspects of vegetation development and condition are best correlated with grain yield. We will then attempt to deduce these important features by calculations using the Vegetation Canopy Reflectance Model. The final step in the development of a yield model is the substitution of the Growth Model values of vegetation development by the Reflectance Model indicators of these values. The result is a model for predicting yield which is dependent only on sequential spectral reflectance values. The steps toward producing a calibrated yield model are shown in Figure 1-a. The Growth Model and the Reflectance Model will be used to develop the functional forms, $f_i(\rho)$, and a relatively small sample of satellite data and associated field-determined grain yield data will be used to calibrate the model by fixing the values of a_i.

---

[16] Colwell, J., 1973, "Bidirectional Spectral Reflectance of Grass Canopies For Determination of Above Ground Standing Biomass", Ph.D. Dissertation University of Michigan, Ann Arbor, Michigan

[17] Welbank, P.J., S.A.W. French, and K.J. Witts, 1966, "Dependence of Yields of Wheat Varieties on Their Leaf Area Durations", Annals of Botany, N.W. Vol. 30, No. 118.

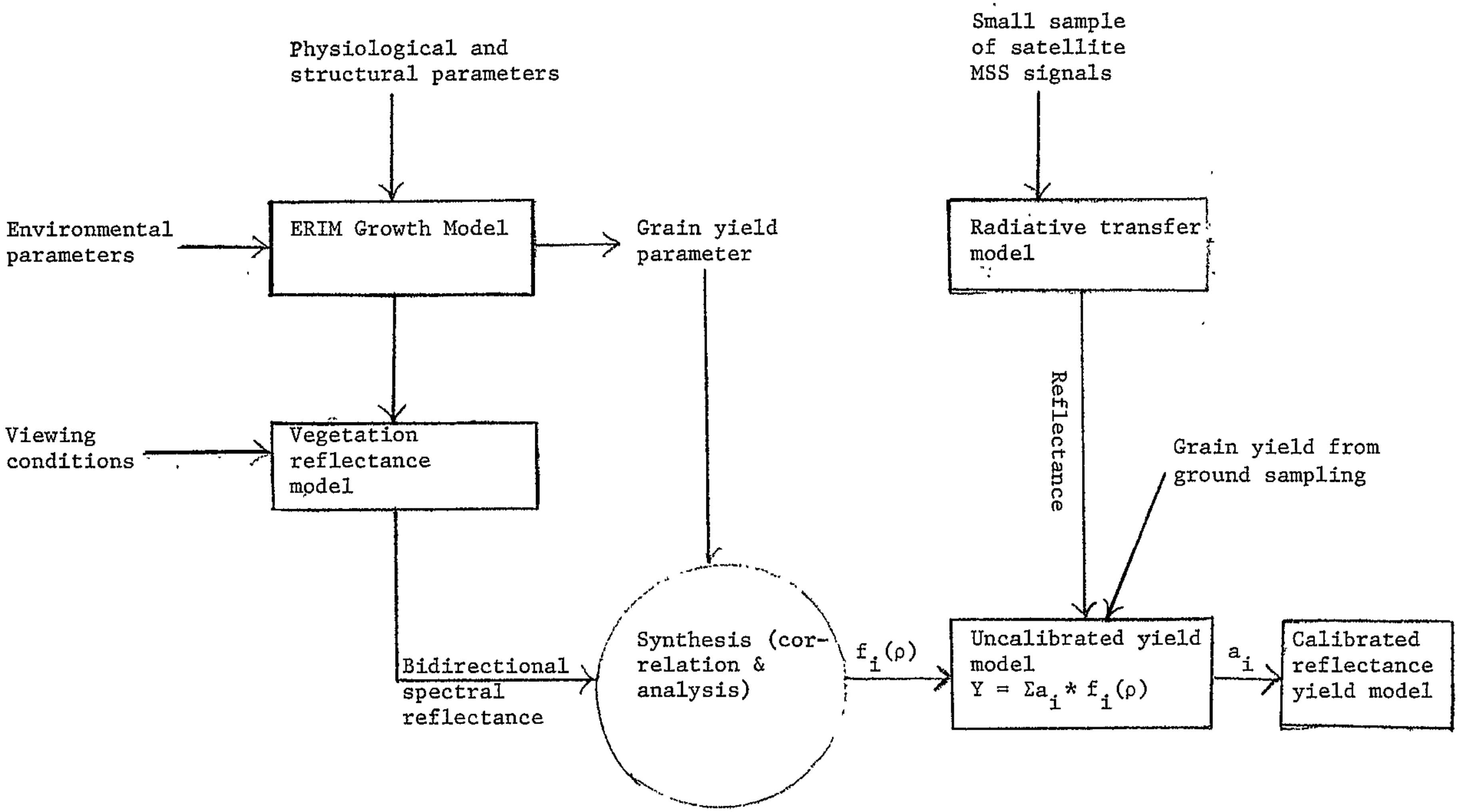

FIGURE 1a. THE RELATIONSHIP BETWEEN ERIM GROWTH MODEL, VEGETATION REFLECTANCE MODEL, AND YIELD MODEL.

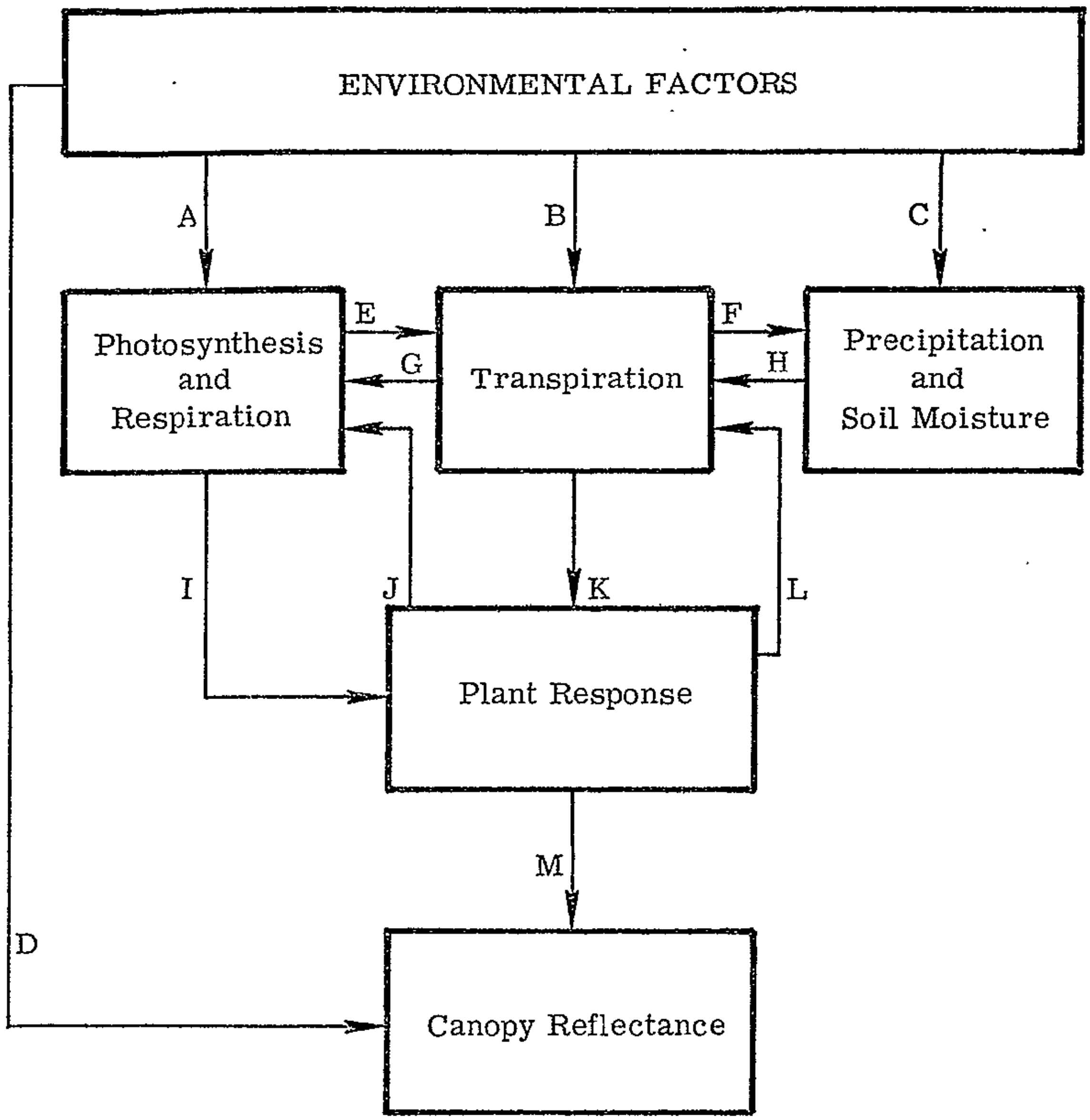

FIGURE 1.

SCHEMATIC DIAGRAM OF THE LOGICAL STRUCTURE
OF THE ERIM GROWTH MODEL

3
GROWTH MODEL DESCRIPTION

The ERIM Growth Model includes two classes of causative factors -- genetically related factors and environmental factors. The combination of these factors is used each hour or day of growth to produce a response or consequence. Such a response changes the influence of the prevailing environmental factors as can be expected from changes in size and structural features of the canopy and from soil moisture depletion. The next response to environmental factors is governed by the consequence of the previous response. The hour-by-hour computation to obtain the next response from the consequences of the previous response simulates the unidirectionality of biological time. The genetically related factors remain fixed.

Figure 1 illustrates schematically the logical structure of the ERIM Growth Model. The boxes represent computations required by the model and the arrows indicate the output of the results of one computation to be used as computational input parameters in another.

Notice that Environmental Factors are wholly driving factors through outputs A, B, C, and D to other computations. It is assumed in this model that the canopy does not influence the local environmental factors significantly, but that such factors are determined by regional influences. The parameters sent through A to Photosynthesis and Respiration are: 1) day type (sunny, partly cloudy, or cloudy); 2) sun angle; 3) diurnal air temperature; and 4) sky and sun irradiance values at the top of the canopy.

The parameters sent through B to Transpiration are diurnal air temperature and dew point for the calculation of air moisture potential. The parameter sent through C to Precipitation and Soil moisture is daily precipitation. The parameters sent through D to Canopy Reflectance are sun angle and day type. Photosynthesis and Respiration for the canopy is calculated utilizing the current canopy structure for intercepting radiation. Stomatal closure due to reduced light level influences transpiration through output E. Daily net production of photosynthate is the output through I to Plant Response. Transpiration is calculated using current soil moisture potential and soil moisture diffusive

resistance using input H and depletes soil moisture by output F. Output G to Photosynthesis and Respiration is stomatal control by leaf moisture potential. Plant Response calculates the allocation of net production of photosynthate to vegetative growth, to storage and to reproductive systems. The translocation process, the slough-off of leaves to the necrotic state, and the geometric orientation of the canopy components are also determined. The appropriate results are returned by outputs J and L.

The output M from Plant Response also provides the spectral class of the canopy components and geometric properties which are required for reflectance calculations. Since canopy reflectance also depends upon the type of illumination, the sun angle and day type are required inputs from D.

One of the results of the Plant Response calculation is moles of fixed CO_2 in the reproductive system. It is this value which is assumed to be proportional to yield. The proportionality factor is discussed in Appendix II.

3.1 PHOTOSYNTHESIS AND RESPIRATION

The primary source of free energy of the canopy is the utilization of solar radiation in photosynthesis. Thermal radiation equilibrium between the canopy and the terrestrial environment is assumed to exist otherwise. Transpiration is driven by the free energy difference between soil moisture and the moisture potential of the surrounding air.

The photosynthesis model we are using is that of Lommen, et.al.[5]. It incorporates the nonlinear influences of both illumination level and temperature on the expected respiration rate and net photosynthesis of 1 cm^2 area of a single leaf. The values of many of the parameters in the photosynthesis model were available from published data. Values of other parameters which were not known precisely were derivable by adjusting them so that the photosynthesis model accurately simulated the results of experiments on photosynthesis of wheat[18].

The geometric properties of the canopy are important both to the calculation of incoming radiation as well as to the calculation of the reflected radiation that serves as the remote sensing link. The assignment of photosynthate to the

[5] Lommen, P.W., C.R. Schwintzer, C.S. Yocum, and D.M. Gates, 1971, "A Model Describing Photosynthesis in Terms of Gas Diffusion and Enzyme Kinetics", Planta (Berl.) 98, 195-220.

[18] Stoy, V., 1965, "Photosynthesis, Respiration, and Carbohydrate Accumulation In Spring Wheat in Relation to Yield", Physiologia Plantarum Supplementuna, IV.

production of new tissue is done so as to create the expected morphological features which are related to the interception of radiant energy.

A portion of the intercepted radiation is the source of photosynthetic free energy. Because of the nonlinear response of photosynthesis to light level, the upper portion of a dense canopy will generally respond quite differently from the lower portion. In addition, the leaf orientation will also influence the illumination level and, hence, the photosynthetic activity. Accordingly, the illumination level at each hour of the day is calculated for the various leaf orientations and leaf locations within the canopy. Five different depths within the canopy are considered for this purpose. The same fundamental concepts are used here as are used in the calculation of reflected radiation from a canopy [1]. Only those particular features of plant morphology which influence the interception and reflection of incoming radiation need to be considered for this aspect of the problem.

This is done by simulating the morphological features of the plant as horizontal and vertical components. Such a procedure leads to quantities which will be called projected leaf area indices (see Fig. 2). The sum of the horizontal and vertical projected leaf area indices will be called the total projected leaf area index, and will be symbolized as PLAI.

The projected leaf area index is not the same thing as biological leaf area index, which is the total one-sided surface area of leaves per unit area of ground. However, the two parameters are probably highly correlated for a given kind of vegetation. There are several advantages to using projected leaf area indices rather than biological leaf area indices for this investigation. Using projected areas allows us to simulate the structure of the crop, at least in a coarse sense. This capability is important both for accurately simulating the irradiance conditions impinging on the canopy as well as for simulating the radiance coming from the canopy.

[1] Suits, G.H., 1972, "The Calculation of the Directional Reflectance of a Vegetative Canopy", Remote Sensing of Environment, V. 2, pp. 117-125.

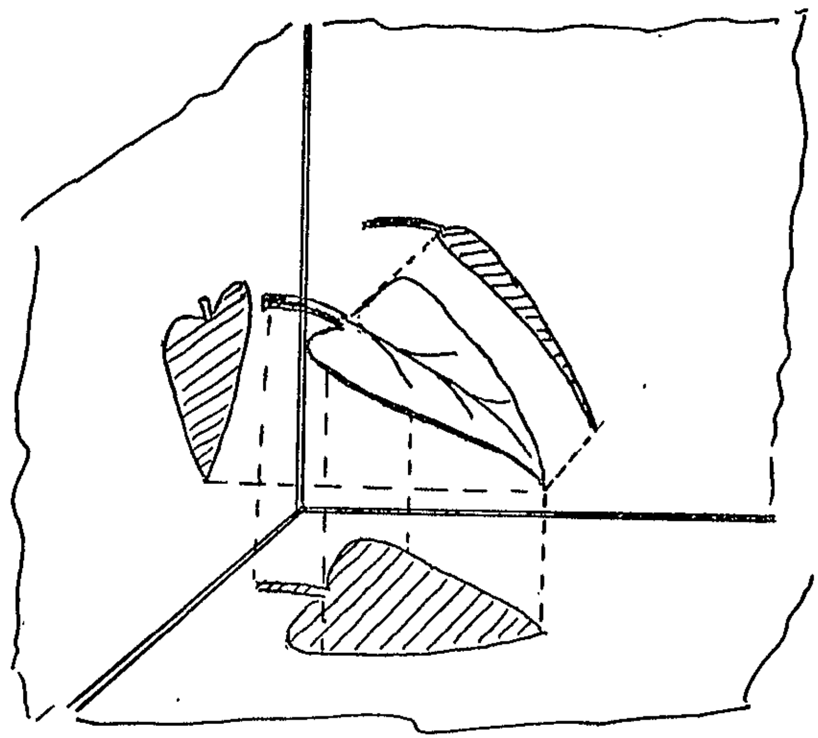

FIGURE 2. ORTHOGONAL PROJECTIONS MAKING IDEALIZED BIOLOGICAL COMPONENTS. The Horizontal Projections Taken Together Lead To A Quantity Called The Horizontal Projected Leaf Area Index. The Vertical Projections Taken Together Lead to a Quantity Called The Vertical Projected Leaf Area Index. The Sum of All of the Projections Defines The Total Projected Leaf Area Index (P.L.A.I.).

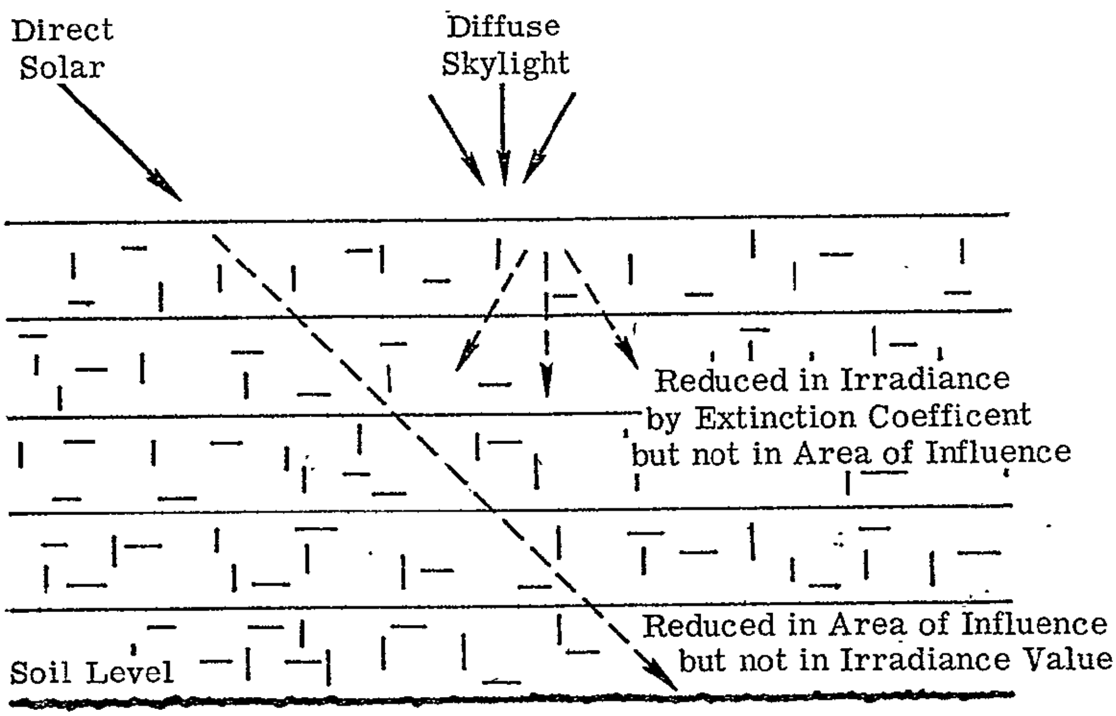

FIGURE 3. SCHEMATIC DIAGRAM OF RADIATION DRIVING PHOTOSYNTHETIC PROCESS IN CANOPY

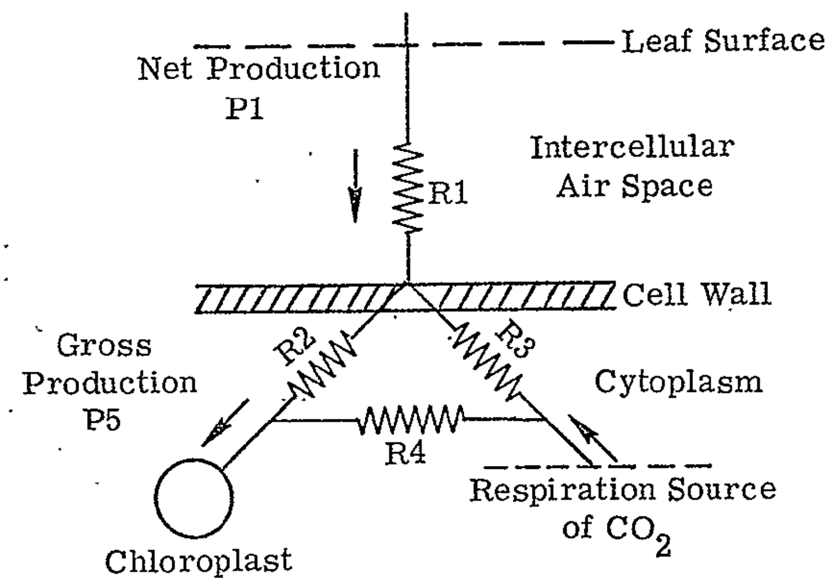

FIGURE 4. SCHEMATIC FLOW DIAGRAM FOR PHOTOSYNTHESIS PROPOSED BY LOMMEN Et Al. FOR UNIT AREA OF LEAF

In addition, a significant amount of photosynthesis is done by components of the canopy other than the leaf laminae which generally are used to define biological leaf area. All of the photosynthesizing area of the canopy will be included in our description of projected leaf area index, unless explicitly stated to the contrary. A finer breakdown of these components is discussed later in this report.

Figure 3 illustrates the idealization of the crop canopy as it functions to intercept, absorb and reflect incident radiation. It is necessary to divide the photosynthetic contributions into a variety of parts to account for the nonlinear response to incident radiation levels. Skylight irradiance decreases with depth of penetration into the canopy, but all components are irradiated. Direct solar irradiance does not decrease, but only the fractional areas of irradiation are decreased with depth of penetration.

Figure 4 illustrates the diffuse flow diagram of CO_2 in photosynthesis as published by Lommen, et.al.[5]. The serrated lines represent diffusive resistances, and P1 and P5 represent diffusive flow rates. The respiration in this portion of the model proceeds at a rate governed by vegetative growth rate and by leaf temperature and illumination. Respiration represents the combined loss of free energy expended in performing the various functions such as cell maintenance, translocation, cell multiplication and expansion.

The fact that the respiratory energy is not allocated entirely in accordance with each particular activity may require correction. Preliminary calculations indicate that the parameter controlling the magnitude of respiration may be the most sensitive parameter of the entire Growth Model. Since the various activities are not necessarily in steady progress at the same time, the observable portions of the canopy may change at noticeably different rates and in this way influence the progression of reflectance values.

3.2 TRANSPIRATION

The schematic diagram of Figure 5 shows the logic of the transpiration calculation. The boxes represent moisture potentials and the serrated lines

[5] Lommen, P.W., C.R. Schwintzer, C.S. Yocum, and D.M. Gates, 1971, "A Model Describing Photosynthesis in Terms of Gas Diffusion and Enzyme Kinetics", Planta (Berl.) 98, 195-220.

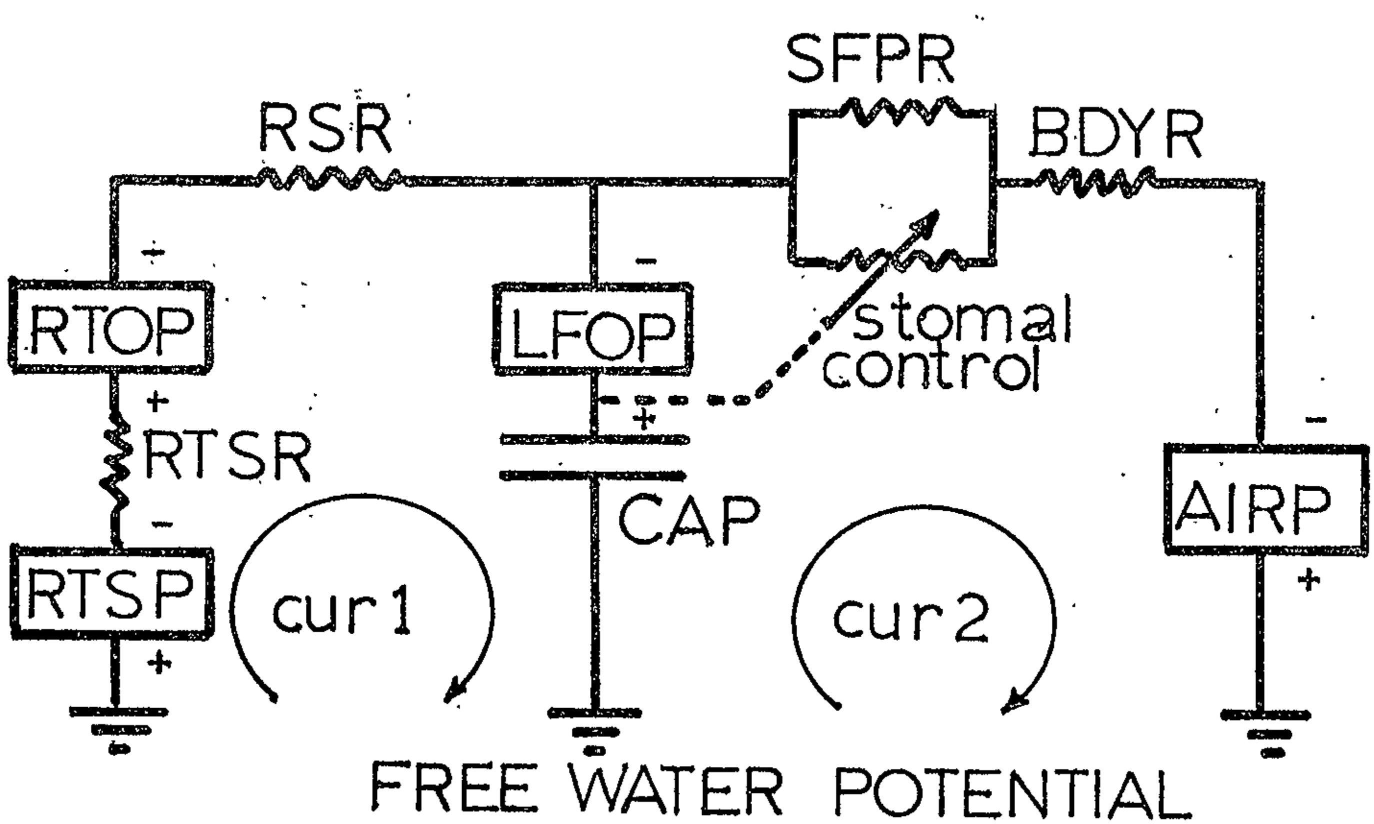

FIGURE 5. XYLEM SYSTEM

represent resistances to moisture flow. The parallel lines designated as CAP represent the total capacity of a plant to retain water under a turgor pressure. Two different moisture currents are considered. CUR1 from soil through roots and stalk to leaf cells is a capillary flow, and CUR2 from cells through the leaf surface to the air is a diffusion flow. CUR1 is the loss of water from the soil, and CUR2 is the loss of water to the air. The soil moisture potential, RTSP, is governed by soil properties and by soil moisture concentration. RTSR, the soil resistance, also depends upon soil properties and soil moisture concentration. RTOP is the root-soil interface osmotic potential and has been considered a small fixed value in calculations to date. RSR is the root and stalk capillary resistance combined. This resistance is assumed to change with plant growth so that the resistance of the root and stalk is reduced in proportion to the projected leaf area of the plant. It is assumed that new capillary pathways are created to accommodate the expanded projected leaf area.

The leaf osmotic potential, LFOP, depends inversely upon the amount of moisture contained in the cell while the turgor pressure is proportional to the amount of moisture within the cell. The algebraic sum of these two potentials is the leaf moisture potential. Stomatal closure is governed by the amount of moisture within the cell. The turgor pressure also controls the leaf orientation. In the present Growth Model the morphology of wilt begins at about 3 bars turgor pressure, and complete wilt occurs at 0 bars.

The surface parallel resistance, SFPR, represents high resistance alternate pathways from the cell to the outside surface of the leaf. The boundary layer resistance, BDYR, completes the moisture pathway to the air which draws moisture due to the air-moisture potential, AIRP.

3.3 PRECIPITATION AND SOIL MOISTURE

A flow chart indicating the way that precipitation and soil moisture are determined is presented in Figure 6. A statistical precipitation model was developed so that 10 or 20 year growth histories can be computed at very low cost. The use of a statistical precipitation model permits introduction of realistic alterations in climate simply by altering the long term averages for the region. Precipitation is zero unless a cloudy day occurs. When a cloudy day does occur,

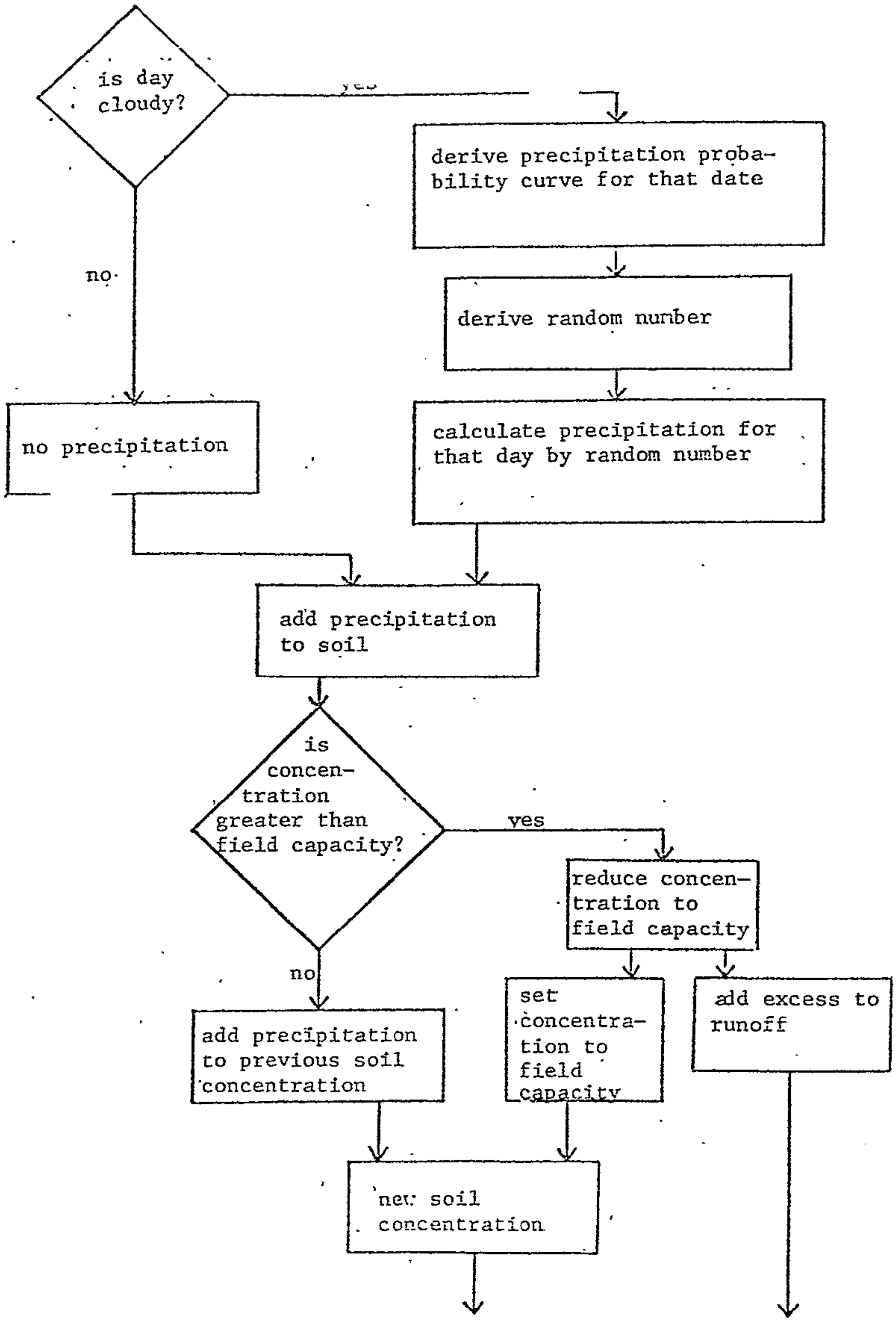

FIGURE 6. FLOW CHART FOR PRECIPITATION AND SOIL MOISTURE

the amount of precipitation is chosen by random number choice in such a way that the greatest rainfall recorded for that month in the geographic region cannot be exceeded and the long term average rainfall reported for that month will result after many trials. The result is a day-to-day precipitation pattern which resembles the frequency and magnitude of rainfall reported by the weather station for that region.

Precipitation is accumulated in the first meter of soil depth. If soil moisture concentration exceeds the field capacity for the soil, run-off or gravitational drainage of the excess occurs. Plant transpiration also removes moisture from the soil. The soil moisture is assumed to be evenly distributed in a fixed thickness of soil (1 meter soil depth in present calculations) without any change in soil properties with depth. Soil moisture extraction is assumed to take place evenly within this region. More realistic root-soil relations are exceedingly complex and sweeping simplifications are required in order to maintain a tractable model. The major requirement of the soil moisture portion of the model is to require accountability of the available moisture and to induce moisture stress morphology as soil moisture is depleted.

3.4 PLANT RESPONSE

Plant Response calculates the allocation of net photosynthetic production to vegetative growth, "vacuole storage", or reproductive organs. In the event that respiration exceeds production of photosynthate, the difference is made up by depletion of "vacuole" storage. During the vegetative growth phase a depletion of vacuole storage below some fixed fraction of the biomass results in suspension of vegetative growth until vacuole storage has been resupplied. If vacuole storage falls still farther, leaf slough-off occurs with the translocation of remaining storage into the rest of the plant. A change in dimension due to water loss and a change in orientation of the necrotic part is specified as required by the morphology of necrosis. The presence of such necrotic tissues in the canopy forms an important part of the remote sensing link. According to this model, two different circumstances can induce leaf slough-off. Extensive moisture stress causes stomatal closure resulting in a reduction of production

and an excess expenditure of storage, which may result in slough-off. In the absence of moisture stress, a growing upper story of the canopy shades the lower portion resulting in a reduction of production and an excess expenditure of storage, which may result in slough-off.

During normal vegetative growth, photosynthesis in excess of storage requirements is allocated to an increase in the biomass. The precise manner in which this allocation is made will very likely be different for different varieties. For purposes of exploring the consequences of the current model, a simple allocation system was used. The projected leaf area index of the canopy was assumed to be proportional to the biomass. The proportionality constant represents the allocation proportions between producing area and non-producing (support) organs. Preliminary calculations indicate that the results are moderately sensitive to the value of this constant. A value was used which appeared to be consistent with published results [19]. Further model refinement in this allocation may be required since the consequences affect both producing area and also vital components of the remote sensing link.

The leaf orientation is also related to the particular morphology of the wheat variety and to age of the plant. Three kinds of orientation are required -- the normal orientation of healthy vegetative growth, the orientation sequence of wilt due to moisture stress, and the orientation of leaf necrosis. Orientation is expressed, in an idealized fashion, as the ratio of total projected leaf area to the total horizontal projections of leaf area within the canopy. Previous field measurements of the orientation of one variety of wheat [20] were used as a guide for preliminary calculations.

3.5 ENVIRONMENTAL FACTORS

The environmental factors affecting the growth of the crop may be introduced from recorded data or by simulation. The above model was operated with simulated environmental data.

[19] Strebeyko, P., M. Wislocka, and T. Krzywacka, 1963, "Dynamics of Growth and Development in Spring Wheat", Physiologia Plantarum, Vol. 16.

[20] Safir, G.R., G.H. Suits, and M.V. Wiese, 1972, "Application of a Directional Reflectance Model to Wheat Canopies Under Stress", Presented at International Conference on Remote Sensing in Arid Lands, Tuscon, Arizona.

The sun angle for a particular latitude is easily computed if one assumes that the earth's orbit is circular with a yearly period of 365 days. The noon sun angle from zenith oscillates about the equinox position in a simple harmonic fashion. The diurnal variation of sun angle is calculated for each day using trigonometric relations. Thus,

$$\eta = \pi/2 + .410*\cos(2\pi*(ND+10)/365)$$

is the relation for the angle in radians of the sunlight direction from the north pole direction on day number, ND, with ND=1 on January 1. The number .410, is the angle 23.5 degrees expressed in radians.

The local polar angle, θ, of the sun as a function of the hour of the day, NH, and latitude of location, ψ, is then

$$\cos\phi = \sin\eta\cos\psi\sin(2\pi(NH-6)/24) + \cos\eta\sin\psi$$

Midnight is given by NH = 0.

The solar illuminance (400-700 nm), ESN, normal to the suns rays in kl/m^2 is calculated from the relation,

$$ESN = 138.8 \exp(-.158/\cos\theta).$$

This relation accounts for some atmospheric attenuation as the sun approaches the horizon. The relation was determined by curve fitting data in graphical form from ITEK [21]. ESN is restricted to positive values.

Clear day sky light illuminance, ESKY, in kl/m^2 was similarly obtained by curve fitting. In addition, the sky is assumed to be uniform and Lambertian. Thus,

$$ESKY = 113.8\ (\pi/2 - \theta)\exp(-2.29(\pi/2 - \theta)) + 6.75$$

where ESKY is restricted to positive values. The twilight condition is incorporated in the relation for ESKY.

Three types of daily weather are considered: sunny, partly cloudy, and cloudy. Illumination conditions for cloudy skies, ECLO, are derived from the

[21] ITEK, 1965, Photographic Considerations for Aerospace, p. 15.

above illuminance values by assuming that a cloud layer, on the average, transmits luminous flux as a plane Lambertian diffuser with a hemispherical transmittance of 0.1. Thus,

$$ECLO = .1(ESKY+ESN*\cos\theta)$$

A partly cloudy day is taken as one where the cloud cover is exactly half cloudy and half sunny every hour.

The choice of day type is presently obtained by pseudo random number selection in such a way that the 10 year averages match the proportions desired. The pseudo random number series (one number for each day) is initiated by the date of the year, e.g., 1961. In this way, the same weather sequence is used for all calculations of a given year.

The mean daily temperature, TM, is assumed to vary harmonically about the mean annual temperature, TMB, for the year for a given geographic region with a seasonal amplitude, TMA. Thus,

$$TM = TMA*\cos[2\pi(ND-NDM)/365] + TMB$$

Where NDM is the day number when the mean temperature reaches maximum. The diurnal temperature (T1) variation around the mean depends upon the day type. The amplitude of diurnal variation for a partly cloudy day, AMPA, is increased for a sunny day by the quantity, AMPR, and is decreased by the same amount on a cloudy day. Thus,

$$T1 = TM+[AMPA+AMPR*(NSW-2)]\cos[2\pi(NH-15)/24]$$

where NSW is 1 for cloudy day, 2 for partly cloudy, and 3 for sunny day. NH is the hour number.

The maximum diurnal temperature occurs at 1500 hours (3 p.m. sun time). The values of AMPA and AMPR can be made consistent with historical weather data. In the present arrangement, no fluctuations in the yearly mean temperature are permitted.

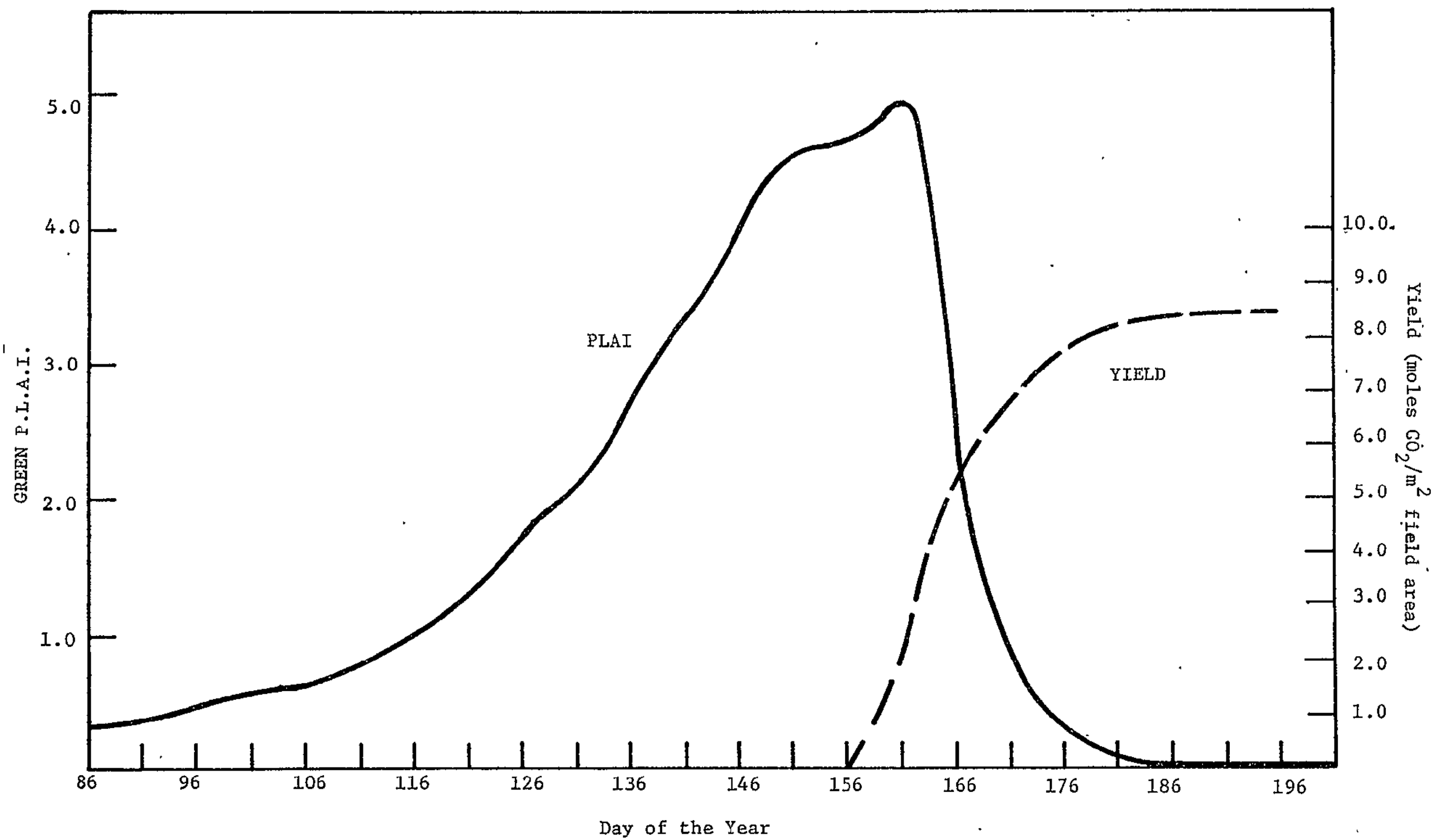

FIGURE 7. SEASONAL GREEN PLAI AND YIELD OUTPUTS OF GROWTH MODEL.

4
GROWTH MODEL RESULTS

A sample of the green projected L.A.I. and yield outputs from the Growth Model is shown in Figure 7. The vegetative growth phase approximates the typical S curve. Deviations from a smooth curve are due to a chance sequence of favorable or unfavorable days. The reproductive activity occurs near the top of the vegetative growth phase where a fall-off in projected leaf area index begins. The rate of this fall-off is highly dependent on the rate of translocation of stored carbohydrate. Details of the hourly performance of the model during several days in the growing season are presented in Appendix III.

In order to assess the performance of the Growth Model under varying environmental conditions, the Growth Model was exercised for four drastically different hypothetical climates and initial values of soil moisture. The results were then analyzed with respect to the relationships between vegetation condition and yield. It was found that there was a direct correlation between green projected leaf area index at the time of heading and final grain yield. This is not unexpected, since the amount of grain produced is a function of the amount of functioning photosynthetic material present.

There is some indication from the literature that there is a good correlation between the summation of the green photosynthetic area over time and final yield. This is particularly true during the period after heading [17]. The summation of the green photosynthetic area may be approximated by the projected leaf area duration (PLAD), defined here as the summation of the daily projected leaf area index over the number of days of interest; i.e.,

$$\text{PLAD} = \sum_{i=1}^{n} \text{PLAI}(i)$$

where PLAI (i) is the projected leaf area index for day i.

The projected leaf area durations after heading for the four hypothetical sets of environmental conditions mentioned above were computed and compared with

[17] Welbank, P.J., S.A.W. French, and K.J. Witts, 1966, "Dependence of Yields of Wheat Varieties on Their Leaf Area Durations", Annals of Botany, N.S. Vol. 30, No. 118.

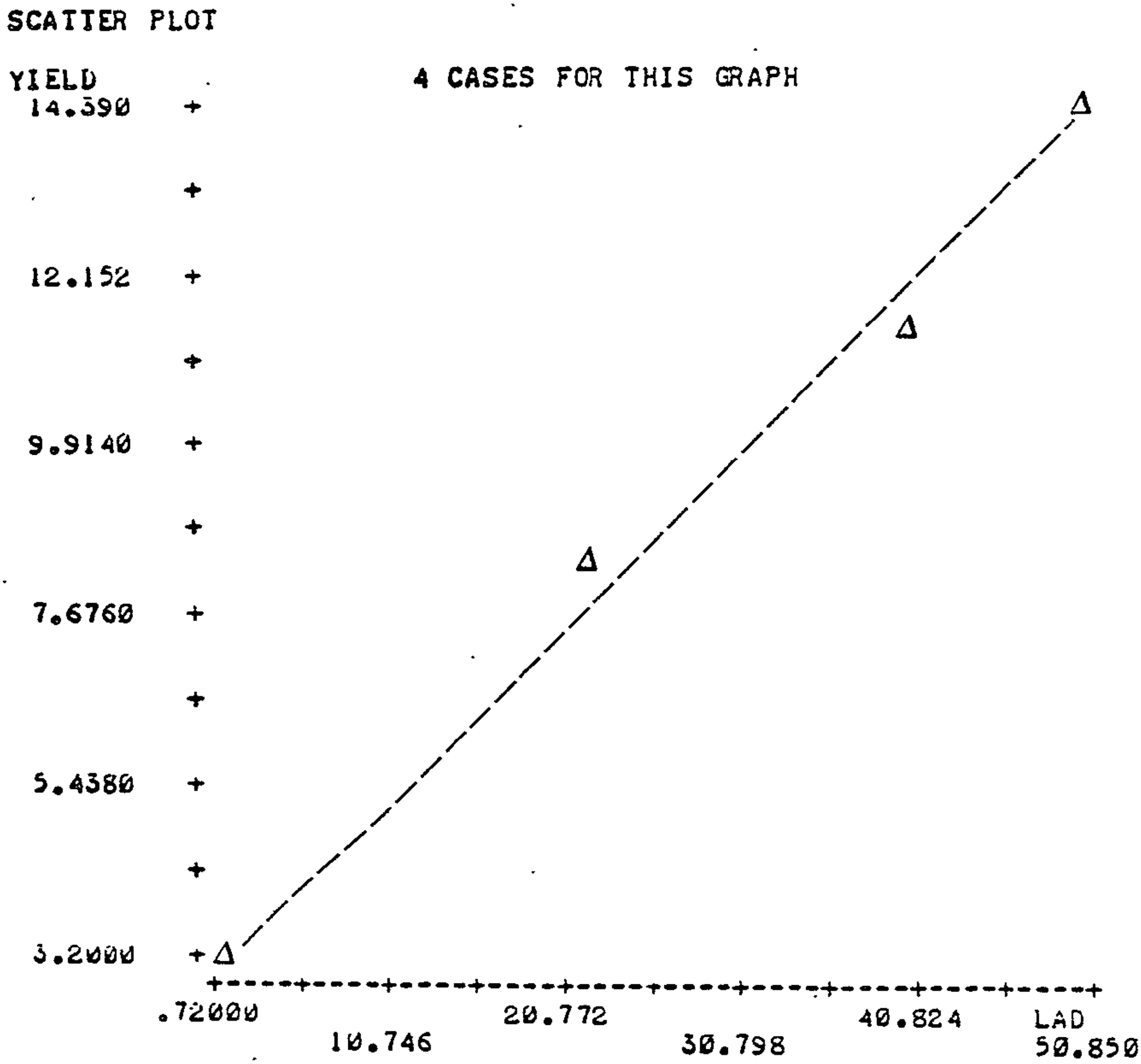

FIGURE 8. RELATIONSHIP BETWEEN PROJECTED LEAF AREA DURATION (PLAD) AND YIELD FOR FOUR PRELIMINARY GROWTH MODEL RESULTS

their corresponding values of yield. The results for the four cases are graphed in Figure 8. As can be seen, for this very limited trial there is an almost linear relationship between projected leaf area duration and wheat grain yield.

These results are very preliminary and on a very small data set, but they suggest that PLAD may be a useful indicator of grain yield. Since PLAI can potentially be approximated using remote sensing data, the results suggest that remote sensing data may be a valuable indicator of wheat grain yield.

In fact, a rudimentary and illustrative yield model based solely on sequential reflectance data can be written based on these results. A simple regression equation can be developed relating yield to projected leaf area duration, and having the form

$$\text{yield} = A + B^* \text{ (PLAD)}$$

For the specific modeled results presented in Figure 8 this equation is

$$\text{yield}_{(\text{moles } CO_2/m^2 \text{ field area})} = 3.24 + .22^* \text{(PLAD)}$$

In addition, a relationship can be established between green PLAI and reflectance data of the form

$$\text{PLAI} = C + D \left(\frac{\rho(750)}{\rho(650)}\right) + E \left(\frac{\rho(750)}{\rho(650)}\right)^2$$

For modeled results of reflectance of a hypothetical crop similar to wheat[16] the above relationship accounted for 95% of the variability in PLAI when using the coefficients.

$$C = 1.17,\ D = -.14,\ E = .017.$$

Simple substitution of radiometric indicators of PLAI for actual PLAI at daily intervals produces a yield model dependent only on periodic reflectance data. The form of the yield model would be

[16] Colwell, J., 1973, "Bidirectional Spectral Reflectance of Grass Canopies for Determination of Above Ground Standing Biomass", Ph.D. Dissertation University of Michigan, Ann Arbor, Michigan.

$$\text{yield} = A+B \sum_{i=1}^{n} C+D\left(\frac{\rho(i,750)}{\rho(i,650)}\right) + E\left(\frac{\rho(i,750)}{\rho(i,650)}\right)^2$$

This yield model is only illustrative of the type of relationship we are attempting to define, and it may have to be modified as a result of future work. The limiting factor to the usefulness of remote sensing data for exploiting the apparent relationship between PLAD and grain yield may prove to be the degree to which PLAD can be approximated from the PLAI estimates available from a limited number of remote sensing observations.

In order to assess the performance of the Growth Model under less drastic variations in environmental conditions, two runs were made with identical climate and initial soil moisture, but with the weather sequence altered. The two weather sequences will be identified as 1960 and 1961. The weather sequence 1961 resulted in 127 sunny days, 120 partly cloudy days, and 119 cloudy days. Total precipitation was 17.19 inches, and runoff or gravitational moisture loss was 6.97 inches. The precipitation for weather sequence 1960 was about 24 inches, but of more importance to plant growth, the precipitation timing in 1960 was more favorable to modeled wheat production. The 1960 modeled wheat required approximately 13" of water for good wheat growth. With the initial soil moisture set at field capacity (20%), the 17 inches of additional precipitation in the 1961 sequence should have been adequate. However, the precipitation arrived at the wrong time, producing runoff instead.

Figure 9 shows the values of computed soil moisture concentration and projected leaf area index of healthy green photosynthetic material at 10 day intervals throughout the growing season. The soil moisture potential in the Growth Model is made to increase rapidly in magnitude at a concentration of 10% (the permanent wilting point), thereby inhibiting growth and production of grain. The relatively high rate of increase of PLAI in the 1961 sequence from days 125 to 145 is due mainly to a period of sunny days with adequate soil moisture. The 1960 sequence increased more slowly over this period due to cloudy days which both conserved and replenished soil moisture. The subsequent more favorable moisture conditions from day 145 to day 155 allowed the 1960 wheat crop to attain a higher peak value of green PLAI. The resulting grain yield in 1960 was more than 50% greater than in 1961.

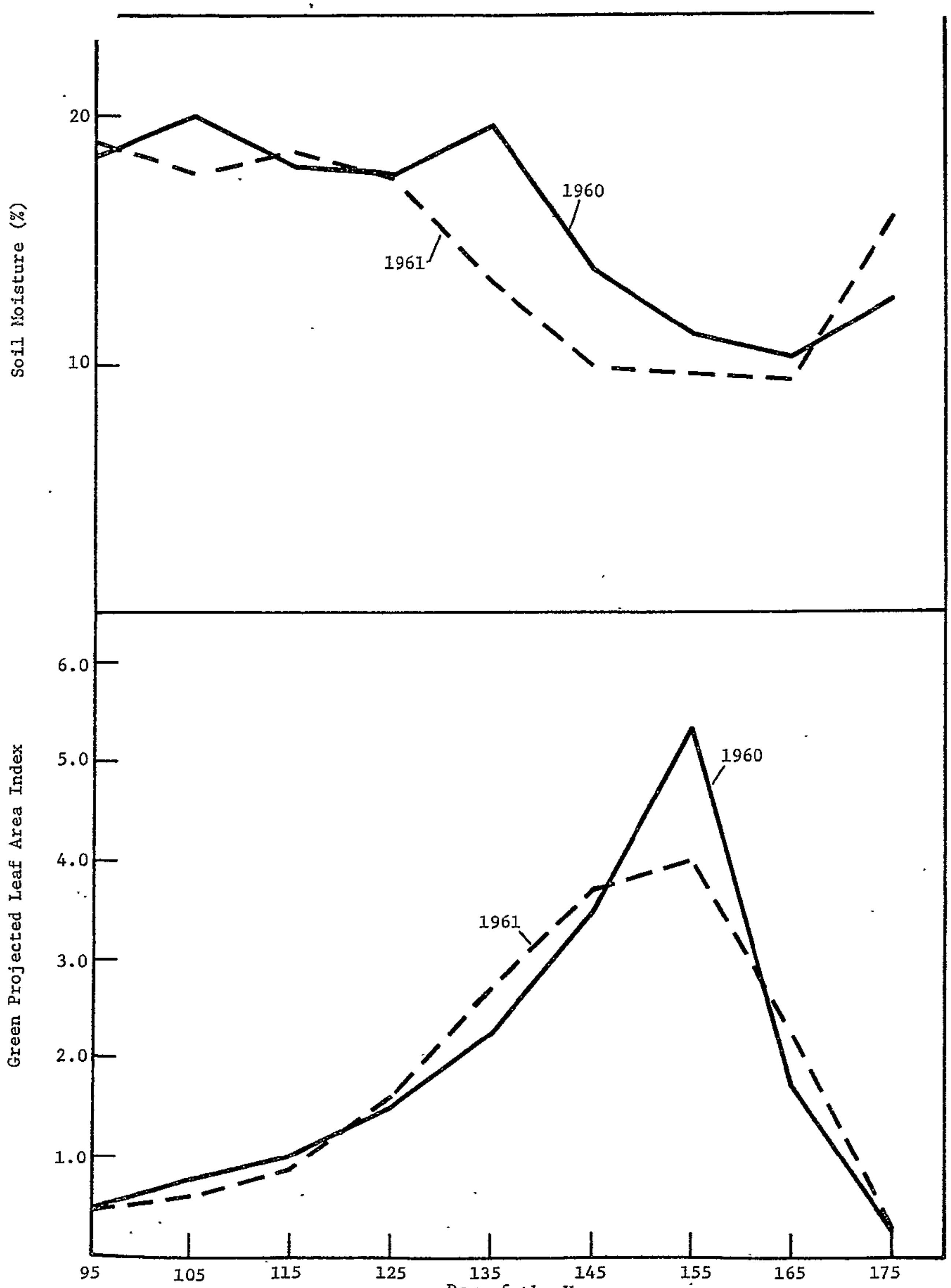

FIGURE 9. Soil Moisture and Green PLAI for two Weather Sequences

5
WHEAT REFLECTANCE MODELING

In order to simulate the sequential bidirectional spectral reflectance of the wheat canopies, it was necessary to devise a strategy for dividing the above ground parts of the wheat canopy into appropriate morphologic and radiometric components (horizontal and vertical projected areas of live and dead leaves and stalks, in two layers.) The specific strategy used is presented in Appendix IV. This strategy is based on data from the literature[19], and on our own observations of wheat. However, it is admittedly a very simplified and coarse strategy that needs refinement. In addition, there was not sufficient time to incorporate this strategy into the Growth Model, so the stategy was applied to the output of the Growth Model. Such a procedure is not strictly correct, since crop characteristics affect the amount of radiation absorbed, as well as other aspects of the functioning of the Growth Model. Nevertheless, this procedure enables us to make calculations of wheat canopy bidirectional spectral reflectance which should be approximately correct, and which permits us to demonstrate the connection between the Growth Model and the Reflectance Model.

The characteristics of the crops simulated for 1960 and 1961 weather sequences which were discussed previously were determined by the strategy in Appendix IV. The resulting projected areas of each type of component (live leaves, dead leaves, live stalks, dead stalks) were used as inputs into a vegetation canopy reflectance model. Previous measurements [20] were used to describe the radiometric properties of the vegetation components and the soil.

The wheat canopy bidirectional spectral reflectance measurements were made for a vertical look angle and a solar zenith angle of 30°. In practice, it would be entirely possible to vary these and other parameters, as appropriate. An example of the bidirectional spectral reflectance which was computed for one day in the 1960 weather sequence is presented in Figure 10.

[19] Strebeyko, P., M. Wislocka, and T. Krzywacka, 1963, "Dynamics of Growth and Development in Spring Wheat", Physiologia Plantarum, Vol. 16.

[20] Safir, G.R., G.H. Suits, and M.V. Wiese, 1972, "Application of a Directional Reflectance Model to Wheat Canopies Under Stress", Presented at International Conference on Remote Sensing in Arid Lands, Tuscon, Arizona.

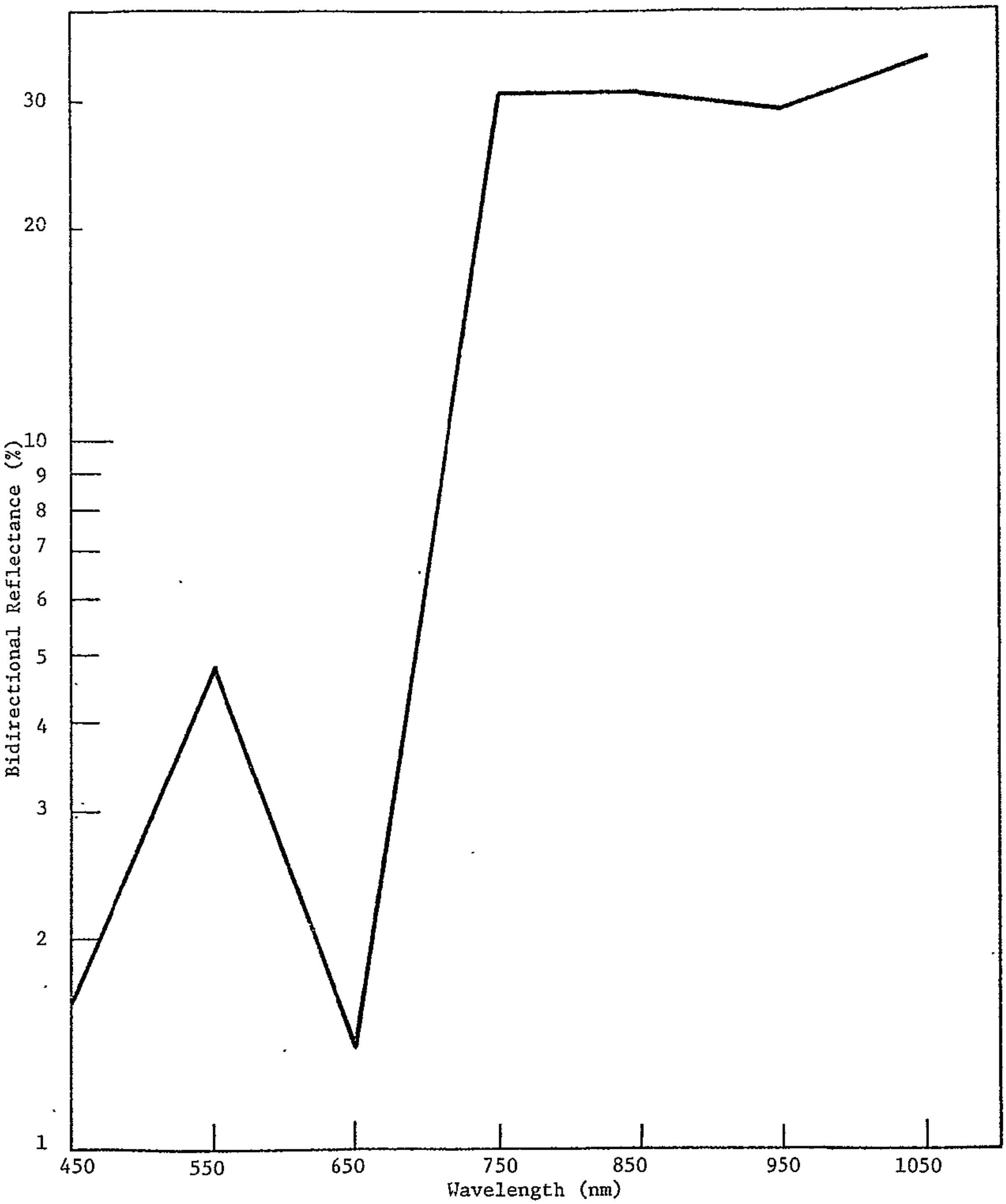

FIGURE 10. REFLECTANCE OF WHEAT CANOPY FOR DAY 155, WEATHER SEQUENCE 1960.

Sequential reflectance characteristics at 10-day intervals for the 1960 and 1961 weather sequences are presented in Figures 11 and 12. The spectral regions shown are 550 nm (green), 650 nm (red), and 750 nm (IR). The reflectance characteristics therefore approximate what could be derived from LANDSAT channels 4, 5, and 6.

The IR reflectance trends for the two seasons can be seen to have approximately the same shapes as the corresponding graphs of PLAI which were presented in Figure 9. This similarity suggests that the trend in vegetation condition can be monitored by appropriate interpretation of LANDSAT Channel 6 data. The red reflectance trends for the two seasons have shapes that are approximately the inverse of the IR reflectance trends and the trends of vegetation development. The relationship of the trends of green reflectance to vegetation development are less clear.

The IR spectral reflectance seems to be the most sensitive of these three spectral regions to vegetation condition, but the red spectral reflectance also has considerable sensitivity to vegetation condition. The green spectral reflectance is not particularly sensitive to vegetation condition.

The inverse relationship between IR and red reflectance with respect to vegetation development suggests that a ratio of these reflectances should be more sensitive to vegetation development than either spectral band separately. IR/red reflectance ratios for the two growing seasons are presented in Figure 13. The additional utility of an IR/red reflectance ratio is that it tends to normalize the effects of varying soil reflectance due to varying soil type and soil moisture. (see Appendix I).

The preceeding discussion suggests that vegetation development can be estimated by appropriate analysis of remote sensing data such as is collected by LANDSAT. Since there also seems to be a relationship between vegetation development and wheat grain yield, LANDSAT data would appear to have the potential to estimate wheat grain yield. What remains to be done is to further refine our understanding of the relationships between vegetation development and yield and between reflectance characteristics and vegetation development. We will then be prepared to formulate a yield model which will predict wheat grain yield by sequential spectral reflectance.

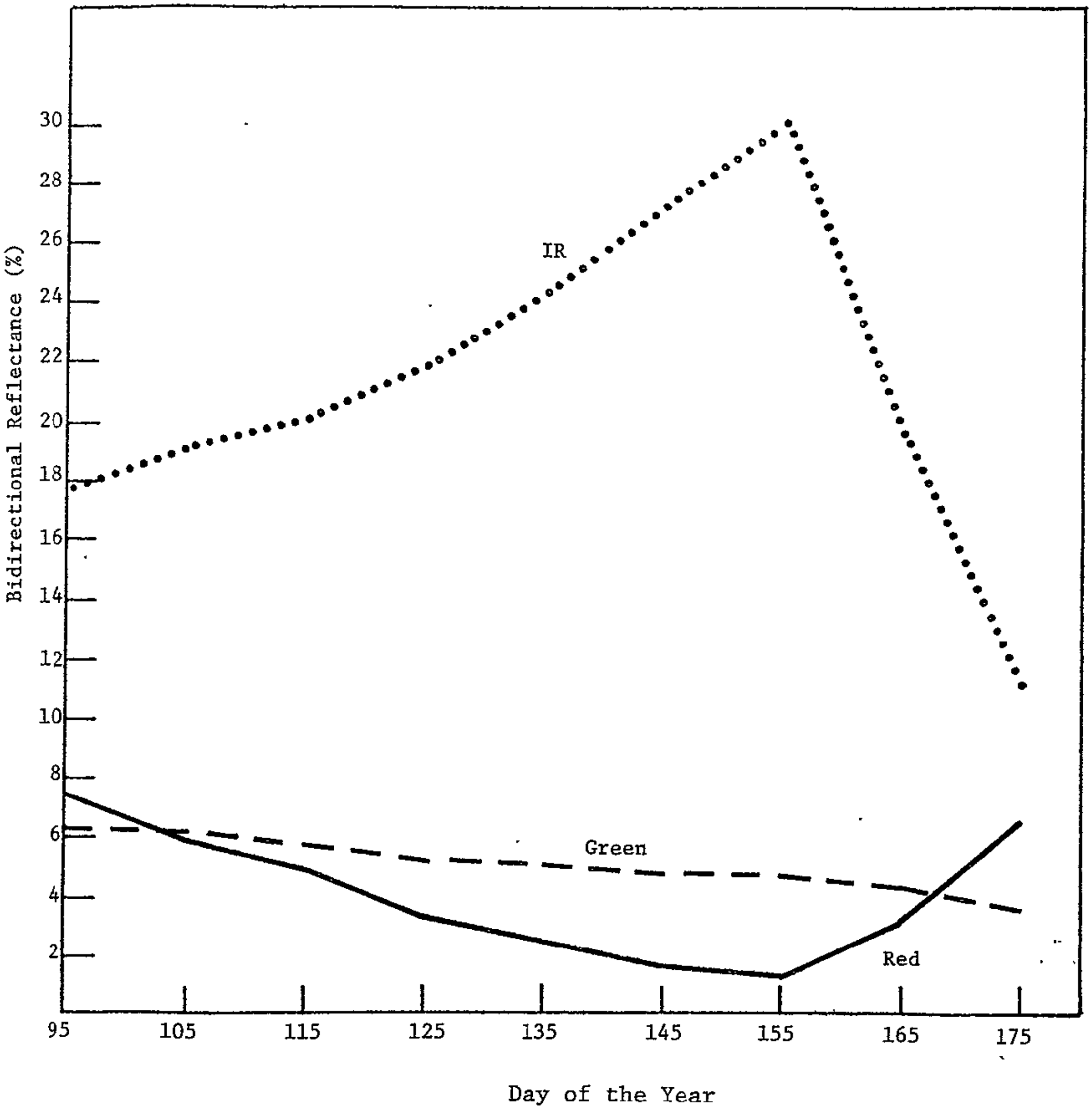

FIGURE 11. WHEAT CANOPY REFLECTANCE IN GREEN, RED, AND IR SPECTRAL REGIONS DURING GROWING SEASON FOR WEATHER SEQUENCE 1960.

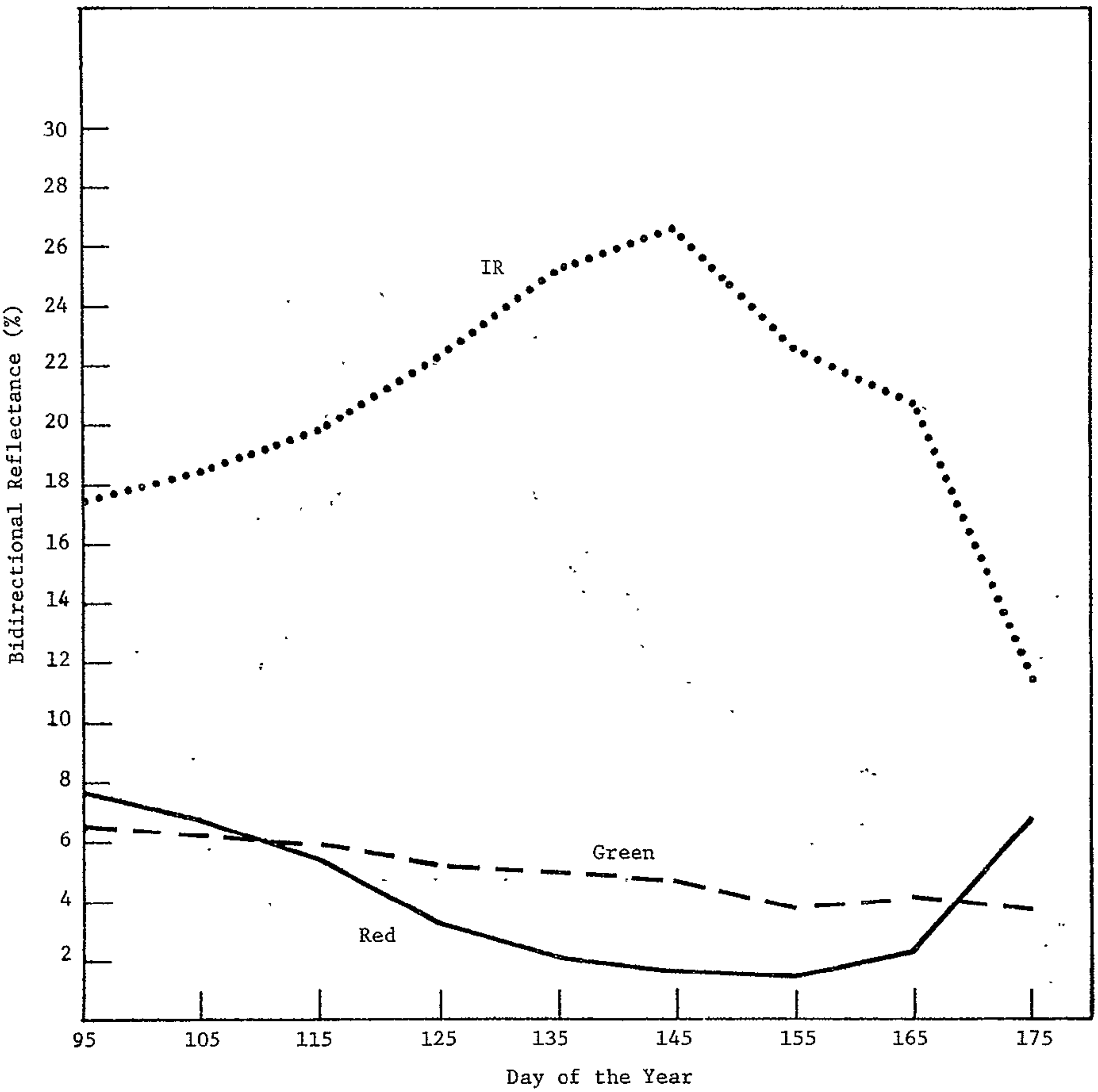

FIGURE 12. WHEAT CANOPY REFLECTANCE IN GREEN, RED, AND IR SPECTRAL REGIONS DURING GROWING SEASON FOR WEATHER SEQUENCE 1961.

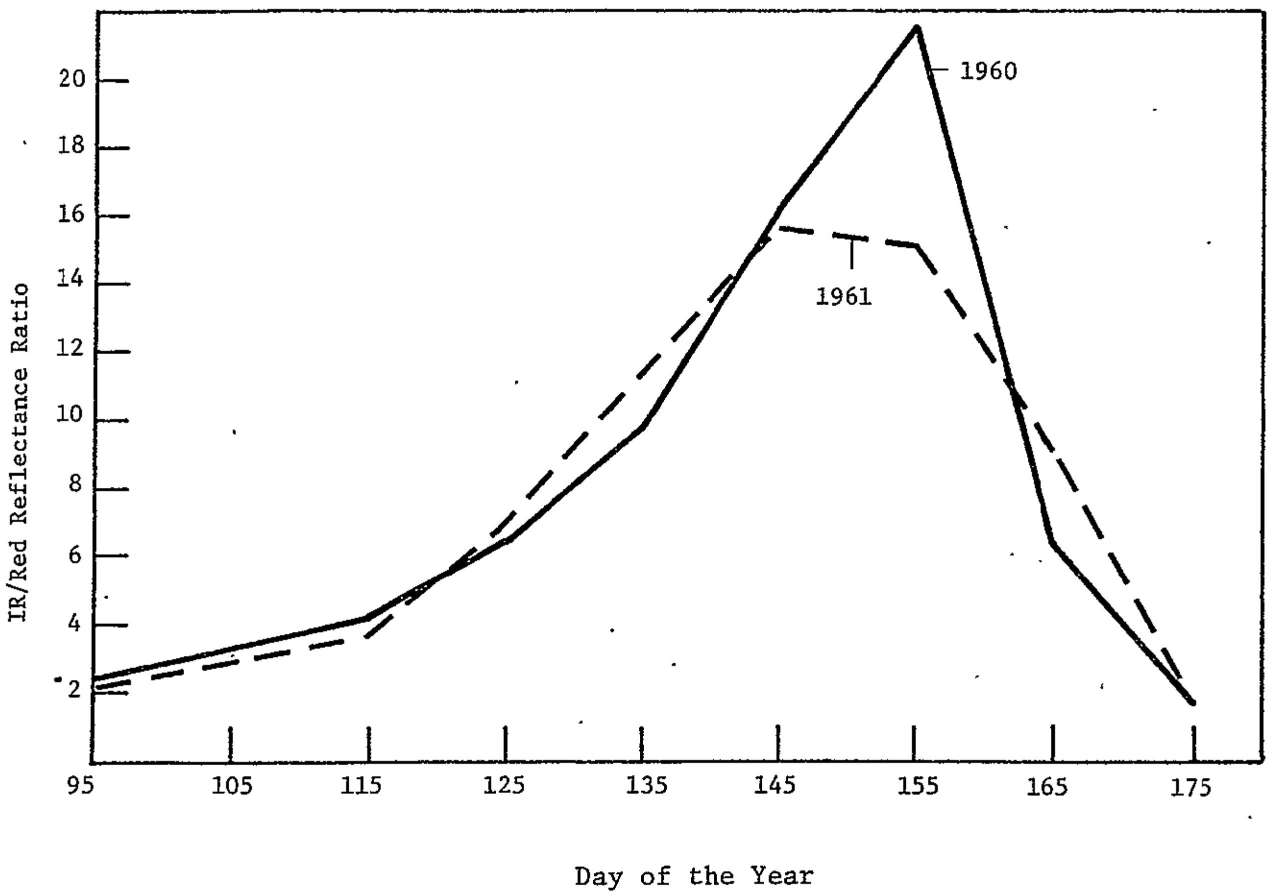

FIGURE 13. WHEAT CANOPY IR/RED REFLECTANCE RATIOS DURING GROWING SEASON FOR WEATHER SEQUENCE 1960 AND 1961.

6
CONCLUSIONS

Any conclusions concerning the significant implications of this effort must be considered as being tentative until validity of the results can be verified by field experiments. Given that fact, the following points seem to be indicated by this effort.

1) Various aspects of wheat vegetation condition are related to grain yield, including peak value of green projected leaf area index, and projected green leaf area duration after heading.

2) Sequential spectral reflectance is indicative of wheat vegetation condition, especially in spectral regions similar to LANDSAT channels 5 and 6 (600-700 nm and 700-800 nm).

3) The degree to which LANDSAT can monitor wheat vegetation condition and forecast grain yield will depend upon both the timing and number of observations available.

4) Water availability and its timing seem to be the most important environmental variables, and information related to water availability would probably enhance the performance of a yield model based primarily on periodic reflectance data.

5) The results of this effort have contributed toward our goal of determining the feasibility of using periodic remotely sensed data to forecast the grain yield of wheat.

7
RECOMMENDATIONS

There are a number of additional things that can be done to facilitate the objectives of this project. Some of the more important ones are listed below:

1) Improve the strategy for describing wheat canopy structure and incorporate into Growth Model.
2) Adjust water relations parameters to those of wheat.
3) Implement differences in diffusive resistance for CO_2 and H_2O for wheat.
4) Adjust translocation parameter values to those of wheat.
5) Test the overall performance of the Growth Model and as many of the subsystems as possible with actual field data.
6) Implement the Growth Model for a variety of weather sequences, climates, and/or other environmental parameters. Compute associated modeled sequential bidirectional spectral reflectances and compare with associated yield in order to derive the functional form of a yield model dependent only upon sequential spectral reflectance. Implement such a model on actual LANDSAT data in order to calibrate the model and assess its performance.

APPENDIX I
EFFECT OF SOIL REFLECTANCE VARIABILITY

The following material addresses some practical problems in using remote sensing data effectively to infer crop characteristics. It illustrates possible solutions to some of the problems, and also shows the value of investigating these problems by a modeling approach. The particular factors discussed include: 1) The effect of variable soil reflectance on vegetation canopy reflectance as a function of a) the percent vegetation cover, and b) the solar zenith angle; plus 2) a possible approach to minimizing the effect of variable soil reflectance by means of ratio processing. Some of the material presented is based on previous work and/or work on other current projects.

The only way it is possible to specify the amount of vegetation present in a canopy using Suits' analytical model is by means of the projected leaf area indices (horizontal, vertical, and total). The ratio of horizontal to vertical projected leaf area indices will be symbolized as H/V, and the reciprocal will be given by V/H.

Percent vegetation cover is the proportion of ground area obscured by vegetation when looking straight down ($\phi = 0°$) at a vegatation canopy. Percent vegetation cover, percent cover, and cover will be used synonymously

Horizontal projected leaf area index is not equivalent to percent vegetation cover. The relationship between the two parameters can be demonstrated by using some of the theory inherent in the reflectance model. A fundamental assumption of the model is that the horizontal components are randomly distributed, an assumption which was confirmed for some of the canopies discussed in this investigation. This random distribution means that leaves can overlap each other. The proportion of vegetation cover [or, alternatively, the probability of at least some vegatative material being in the vertical ($\phi = 0°$) line-of-sight] for a vegetation canopy with horizontal P.L.A.I. = H is therefore given by the negative exponential relationship

$$1-e^{-H}$$

A comparison between some values of horizontal P.L.A.I. and $1-e^{-H}$ is given in Table I-a.

TABLE I-a. HORIZONTAL P.L.A.I. vs. $(1-e^{-H})$

Horizontal P.L.A.I.	$1-e^{-H}$
1	.63
2	.86
3	.95
4	.98
5	.99

Therefore, as one term increases, so does the other, but at a different rate.

Variable soil reflectance can have a substantial effect on the reflectance of a vegetation canopy. Therefore, it is important to understand this effect if we are to infer information about yield from remote sensing of vegetation canopies.

In an attempt to clarify the effect, a number of calculations of vegetation canopy reflectance were made using a canopy reflectance model and two different values of soil reflectance. The canopy reflectance model is the same one which is being used for some of the concepts of the yield model. The complete canopy reflectance model is described by Suits[1]. All canopy reflectance data presented are bidirectional reflectances, with the angle of view being straight down. The results and conclusions may be different at other angles of view, as discussed by J. Colwell[16].

---

[1] Suits, G. H. 1972. "The calculation of the directional reflectance of a vegatative canopy." Remote Sensing of Environment, V.2, pp. 117-125.

[16] Colwell, J., 1973, "Bidirectional Spectral Reflectance of Grass Canopies for Determination of Above Ground Standing Biomass", PhD Dissertation, University of Michigan, Ann Arbor, Michigan.

Effect of Soil Reflectance as a Function of Vegetation Cover

Some of the relevant parameters which were used as inputs to the reflectance model for the following discussion are listed in Table I-b. The spectral regions investigated include the green, red, and near IR. Specifically, the characteristics were chosen to be reasonably representative of the 500-600nm region, the 600-700nm, and the 700-800nm region. The results, therefore, are approximately what would be expected in LANDSAT channels 4, 5, and 6. The structural relationships used [principally the ratio of the projected vertical leaf area (V) to the projected horizontal leaf area (H)] are consistent with physical measurements made on wheat plants by Safir et al[20].

TABLE I-b. HEMISPHERICAL REFLECTANCE AND TRANSMITTANCE VALUES USED IN MODELING FOR VEGETATION COVER

Spectral Region	Percent Vegetation Reflectance	Percent Vegetation Transmittance	Percent Soil Reflectance	
			LIGHT SOIL	DARK SOIL
Green	20.0	25.0	10.0	5.0
Red	5.0	5.0	15.0	5.0
Near IR	50.0	45.0	25.0	10.0

Some of the results are presented in Figures I-a and I-b. As can be seen, there is a considerable difference in vegetation canopy reflectance for the two soil reflectances at low values of projected leaf area index. For example, at a total P.L.A.I. of .325 (vegetation cover of approximately 10%), the canopy with the high reflecting soil has an IR reflectance (LANDSAT channel 6) of 27.2%, and the canopy with the low reflecting soil has an IR

---

[20] Safir, G.R., G.H. Suits, and M.V. Wiese, 1972, "Application of A directional reflectance model to wheat canopies under stress". Presented at International Conference on Remote Sensing in Arid Lands. Tuscon, Arizona.

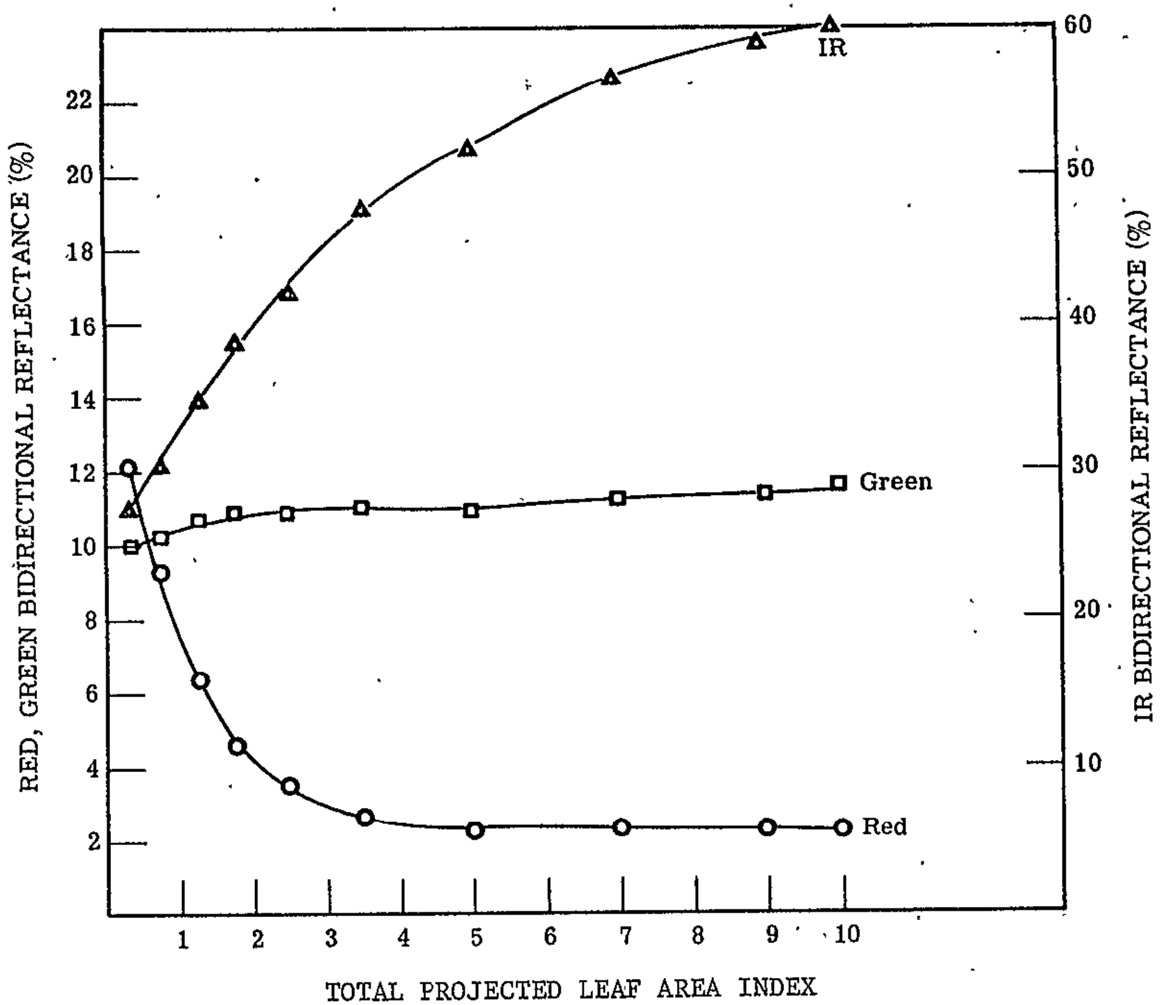

FIGURE I-a. BIDIRECTIONAL REFLECTANCE OF SIMULATED CANOPIES WITH LIGHT SOIL

Solar Zenith Angle, θ = 20°

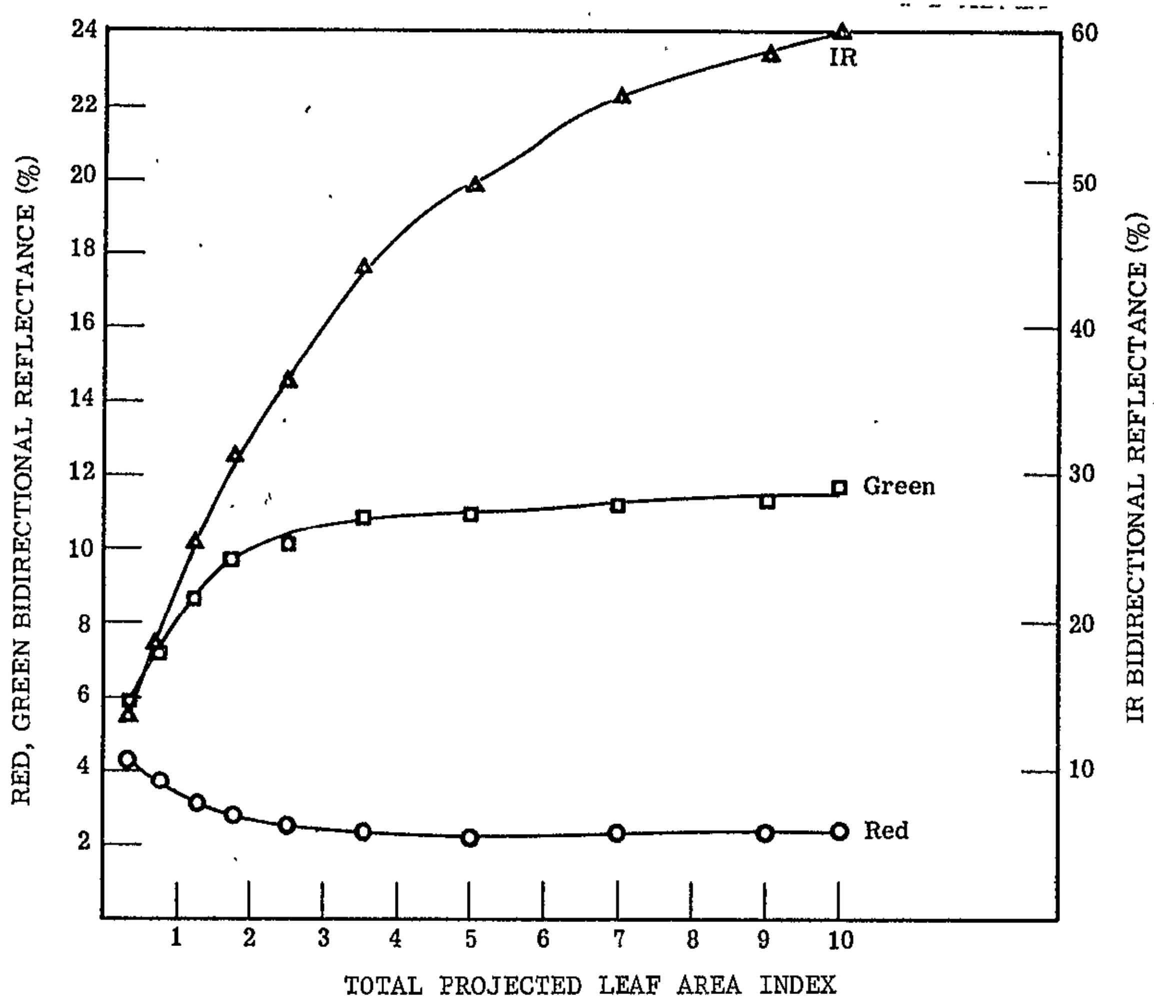

FIGURE I-5. BIDIRECTIONAL REFLECTANCE OF SIMULATED CANOPIES WITH DARK SOIL

Solar Zenith Anlge, θ = 20°

reflectance of 13.5%. Corresponding values for green (channel 4) and red (channel 5) reflectance are given in Table I-c. The canopy spectral reflectance values for a total P.L.A.I. of 5.00 (vegetation cover of 86%) are presented for comparison to show that variable soil reflectance affects vegetation canopy reflectance very little at high values of percent vegetation cover.

TABLE I-c. VARIABILITY OF VEGETATION CANOPY SPECTRAL REFLECTANCE DUE TO VARIABLE SOIL REFLECTANCE AS A FUNCTION OF PERCENT VEGETATION COVER AND P.L.A.I.

TOTAL P.L.A.I.	% Cover $(1-e^{-H}) \times 100$	Green Reflectance (%) Light	Dark	$\Delta\rho$	Red Reflectance (%) Light	Dark	$\Delta\rho$	IR Reflectance (%) Light	Dark	$\Delta\rho$
0.325	10	10.0	5.9	4.1	12.1	4.3	7.8	27.2	13.5	13.7
5.0	86	10.9	10.9	0.0	2.3	2.2	0.1	51.8	49.6	2.2

Empirical data were also collected to investigate the effect of variable soil reflectance as a function of vegetative cover. The data were collected outdoors under nearly clear skies and a solar zenith angle of 40° for canopies of oats that were morphologically similar to wheat. Important canopy parameters are presented in Table I-d. Some of the results are presented in Table I-e.

TABLE I-d. RELATIVE VALUES OF HEMISPHERICAL REFLECTANCE AND TRANSMITTANCE FOR COMPONENTS OF EXPERIMENTAL OATS VEGETATION CANOPIES

Spectral Region	Vegetation		Soil Light	Soil Dark
	ρ	τ	ρ	ρ
Green	17	16	20.3	2.6
Red	6	2	25.1	4.0
IR	47	46	27.2	6.8

TABLE I-e. EFFECT OF SOIL REFLECTANCE ON OATS CANOPY REFLECTANCE AS A FUNCTION OF PERCENT VEGETATION COVER

	Green		Red		IR	
Vegetation Cover (%)	light	dark	light	dark	light	dark
$\sim$10	16.6	2.8	19.8	3.6	25.7	8.1
$\sim$80	6.4	6.7	2.5	2.8	42.3	43.5

The preceding data clearly indicate that soil reflectance can have a significant effect on vegetation canopy reflectance. They also show that the magnitude of this effect is dependent on the percent vegetation cover. This situation makes it very difficult to correct for the effect of soil reflectance without considerable *a priori* knowledge. Without such *a priori* knowledge it can be very difficult to unambiguously infer anything about the *vegetation* from the *canopy* reflectance (which includes the effects of the soil) using single band data.

For example, for the conditions for which the vegetation canopy reflectance modeling was done, light soil with no vegetation (0% cover) is virtually indistinguishable in the near IR band (Channel 6) from a canopy consisting of dark soil and a total projected leaf area index of 1.25 (cover ∿40%). In the red band (Channel 5), dark soil with no vegetation is virtually indistinguishable from a canopy consisting of light soil and a total projected leaf area index of about 1.75 (cover ∿50%).

For the conditions under which the empirical data on oats canopy reflectance were obtained, light soil with no vegetation is virtually indistinguishable in the near IR band from a canopy consisting of dark soil and approximately 50 percent vegetation cover. In the red band, dark soil with no vegetation is virtually indistinguishable from a canopy consisting of light soil and approximately 60 percent vegetation cover.

Effect of Soil Reflectance as a Function of Solar Zenith Angle

The preceding examples illustrate some of the single band ambiguity involved in interpreting characteristics of the vegetation in the presence of soil reflectance variability. Clearly, some means of minimizing the effect of soil reflectance variability (or correcting for it) would be highly desirable.

The solar zenith angle is one of the parameters which determines the magnitude of the effect of variable soil reflectance. As the solar zenith angle increases, more of the soil is shadowed by the vegetation. As a result, there is a decreasing contribution to the vegetation canopy reflectance from the soil, so variations in soil reflectance have less effect on canopy reflectance.

It has been shown that at high percent vegetation cover, the effect of variable soil reflectance is neglibible. Therefore, in showing the effects of solar zenith angle on minimizing variable soil reflectance, it is necessary to use an immature crop (low percent vegetation cover).

For this investigation, immature crops were simulated from data collected by Suits and Safir[22], Safir et al[20] and Suits and Safir (personal communication) on reflectance, transmittance, and structural properties of wheat, sugarbeets, and corn. Since percent vegetation cover (and horizontal P.L.A.I.) has already been shown to have pronounced effects on vegetation canopy reflectance (Figures I-b and I-c), all three types of canopies were made to have approximately the same percent vegetation cover (50%), while still retaining their distinct optical and structural properties.

The effect of solar zenith angle on simulated wheat canopy reflectance is shown in Tables I-f and I-g. Note the decreasing effects of soil reflectance as solar zenith angle goes from 10° to 50° to 70°. The greatest absolute change in canopy reflectance at all solar zenith angles occurs in the IR region because of the greater diffuse flux which results from the generally high vegetation transmittance.

These calculations indicate that the optimum solar zenith angle for minimizing effects of soil reflectance occurs as θ approaches 90° (the horizon). However, it is important to appreciate the ancillary effects that solar zenith angle has on two important functions: 1) crop identification; and 2) crop yield estimation.

The effect of solar zenith angle on the ability to differentiate between various simulated crop types with approximately the same percent vegetation cover is shown in Tables I-f, I-h, and I-i. It can be seen that for these canopies there is a greater difference in reflectance among the

---

[20] Safir, G.R., G.H. Suits, and M.V. Wiese. 1972. "Application of a Directional Reflectance Model to Wheat Canopies Under Stress." Presented at International Conference on Remote Sensing in Arid Lands, Tuscon, Arizona.

[22] Suits, G.H., and G.R. Safir, 1972. "Verification of a Reflectance Model for Mature Corn With Applications to Corn Blight Detection." Remote Sensing of Environment. V. 2 pp 183-192.

TABLE I-f. SIMULATED WHEAT CANOPY REFLECTANCE FOR LIGHT AND DARK SOIL AS A FUNCTION OF SOLAR ZENITH ANGLE, θ

WHEAT

	GREEN		RED		IR	
θ	Light	Dark	Light	Dark	Light	Dark
10°	8.5	5.4	7.4	3.2	36.7	23.3
50°	4.2	3.3	2.5	1.3	27.5	19.8
70°	3.1	2.6	1.3	0.8	23.2	17.3

TABLE I-g. DIFFERENCE IN SPECTRAL REFLECTANCE OF SIMULATED WHEAT CANOPIES WITH LIGHT SOIL AND WITH DARK SOIL AS A FUNCTION OF SOLAR ZENITH ANGLE, θ

$\Delta\rho$(%) (Light - Dark)

θ	Green	Red	IR
10°	3.1	4.2	13.4
50°	0.9	1.2	7.7
70°	0.5	0.5	5.9

crop types at large solar zenith angle (70°) in many of the cases. In general, it appears that the ability to differentiate between crop types of similar percent vegetation cover and horizontal P.L.A.I. but different structure (H/V) is enhanced by large solar zenith angle. This is because at near-vertical look angles the only way the vertical components (which may be the distinctive components) can be "seen" is by means of the shadow they cast. The amount of shadow cast by vertical components approaches a maximum as θ approaches 90°.

These results should be viewed in proper perspective, however. The simulated crops have similar spectral reflectance at small zenith angles because they were made to have approximately the same percentage cover (horizontal P.L.A.I.) They tend to look more dissimilar at large solar zenith angles because large solar zenith angles accentuate the differences in structure (H/V). The exceptions to this trend are probably due to small but significant differences in vegetation cover or canopy radiometric properties. In the real world, however, different crops are planted at different times and develop at different rates, and to different extents (maximum % cover and P.L.A.I.) Accordingly, the most distinguishing feature for most real crops during the growing season is likely to be percent vegetation cover (or components with distinctive radiometric properties), rather than structure. As will be discussed later, differences in percent vegetation cover are frequently not manifest as distinctly at large solar zenith angles, at least at high values of percent vegetation cover. Therefore, in realistic situations large solar zenith angle may actually degrade the ability to differentiate among various crop types.

In addition, it should be noted that the parts of the canopy which furnish the vast majority of the projected area viewed at the near-normal look angles encompassed by a satellite such as ERTS are the horizontal "components" (including the soil). At large solar zenith angle the irradiance on these horizontal "components" is quite small. Therefore,

TABLE I-h. SIMULATED SUGARBEETS AND CORN CANOPY REFLECTANCE FOR LIGHT SOIL AND DARK SOIL AS A FUNCTION OF SOLAR ZENITH ANGLE, θ

SUGARBEETS

	GREEN		RED		IR	
θ	Light	Dark	Light	Dark	Light	Dark
10°	10.2	6.2	9.8	4.2	42.5	26.1
70°	6.3	4.4	4.8	2.5	32.5	22.1

CORN

	GREEN		RED		IR	
θ	Light	Dark	Light	Dark	Light	Dark
10°	9.5	6.6	9.7	5.5	40.7	27.5
70°	4.2	3.8	3.1	2.5	27.4	21.8

TABLE I-i. DIFFERENCE IN REFLECTANCE BETWEEN SIMULATED CROP TYPES FOR LIGHT AND DARK SOIL AS A FUNCTION OF SOLAR ZENITH ANGLE, θ

$\Delta\rho$ SUGARBEETS - WHEAT

	GREEN		RED		IR	
θ	Light	Dark	Light	Dark	Light	Dark
10°	+1.7	+0.8	+2.4	+1.0	+5.8	+2.8
70°	+3.2	+1.8	+3.5	+1.7	+9.3	+4.8

$\Delta\rho$ CORN - WHEAT

	GREEN		RED		IR	
θ	Light	Dark	Light	Dark	Light	Dark
10°	+1.0	+1.2	+2.3	+2.3	+4.0	+4.2
70°	+1.1	+1.2	+1.8	+1.7	+4.2	+4.5

$\Delta\rho$ SUGARBEETS - CORN

	GREEN		RED		IR	
θ	Light	Dark	Light	Dark	Light	Dark
10°	+0.7	-0.4	+0.1	-1.3	+1.8	-4.0
70°	+2.1	+1.7	+2.7	0.0	+5.1	+0.3

the radiance from the canopy becomes quite small. Atmospheric path radiance, on the other hand, has been found to increase steadily from a solar zenith angle of 0° to about 70°[21]. As a result, at satellite altitude the radiance from the canopy may become less than the radiance from the atmosphere in certain spectral bands at large solar zenith angles.

Evidence presented in this report indicates that crop condition and potential yield within a given crop type are associated with P.L.A.I., and hence percent vegetation cover. Therefore, it is important to know how solar zenith angle effects the capability to measure such parameters.

The optimum solar zenith angle for measuring the full range of values of percent vegetation cover and horizontal P.L.A.I. in the spectral regions where soil reflectance is greater than vegetation reflectance (generally green, and red) is 0°. At any other solar zenith angle, canopy reflectance will become nearly insensitive to change in vegetation cover when the <u>combination</u> of sunlit vegetation cover and shadow seen becomes 100 percent (i.e., virtually no illuminated bare soil is seen). On the other hand, when solar zenith angle is greater than 0°, canopy reflectance is probably more sensitive to <u>changes</u> in P.L.A.I. and percent cover in the region where shadow and vegetation seen is less than 100 percent. This enhanced sensitivity results because the drop in reflectance due to increased percent cover will be amplified by increased percent shadow.

Sensitivity to change in percent vegetation cover at low values of percent vegetation cover is generally greatest in the red spectral region due to the high soil/vegetation reflectance contrast, the low transmittance of the vegetation (which produces dark shadows), and the intermediate level (between green and near IR) of skylight irradiance (the only additional source of illumination for the shadowed areas). These factors suggest that the optimum way of distinguishing recently emergent vegetation (~10 percent vegetation cover) from bare soil is to monitor the red band data with the sun at large solar zenith angle (i.e., near the horizon). This procedure might be useful, for example, for early detection of fields planted to winter wheat.

[21] ITEK. 1965. Photographic Considerations for Aerospace, p. 15.

For spectral regions where vegetation reflectance is greater than soil reflectance (generally the near IR), 0° is still the optimum solar zenith angle for differentiating the full range of values of P.L.A.I. and percent cover. On the other hand, any deviation of the solar zenith angle from 0° will decrease the sensitivity over the region where vegetation and shadow is less than 100 percent. This situation suggests that large solar zenith angle is generally the worst condition for early detection of winter wheat in the near IR spectral region.

Since large solar zenith angle appears to have a number of disadvantages for measuring important crop characteristics, other ways of suppressing the effects of variable soil reflectance should be investigated. One possible approach is described in the following discussion.

Effect of Ratioing on Variable Soil Reflectance

Soil reflectance variability is primarily due to either variability in soil type (texture, mineral composition, etc.) or soil moisture. Condit[23] has investigated the effects of the variability in both factors for a sample of major soils types in the United States. This investigation disclosed a very large degree of variability in soil reflectance, even larger than represented in the previous discussion. For example, for dry soils the reflectance at 650 nm varied from 7.5% to 69.5%, and at 750 nm the corresponding figures were 38.2% $\pm$ 16.2%. A general characteristic of the soils, however, is that the reflectance usually steadily increases with increasing wavelength over the visible and near IR region. This general spectral property of soils leads one to suspect that a ratio of signals from adjacent spectral bands may be more nearly independent of soil type than single band signals. Nazare[24] found this to be the case for a large variety of rock types.

Ratios of a number of pairs of spectral bands were computed using Condit's raw data. The ratio of reflectances at 750 nm and 650 nm (IR/Red)

---

[23] Condit, H.R. 1970. "The spectral reflectance of American Soils." Photogrammetric Engineering. V. 36 #9 pp. 955-966.

[24] Nazare', C. 1973. "An analysis of laboratory hemispherical Reflectance Spectra of Selected Rocks in the Wavelength Range 0.35 to 3.50 micrometer." M.S. Thesis, University of Michigan, Ann Arbor, Michigan.

was found to be reasonably constant for all soil types. The mean value for this ratio was 1.19 and the standard deviation was 0.12. The variability within the three general "classes" of soils identified by Condit was even less.

The major cause of soil reflectance variability other than soil type is soil moisture. Accordingly, the reflectance variability for the same soils as a function of whether they were dry or wet has been computed from Condit's raw data. The change in reflectance with moisture content for a given soil type was found to be as great as 22% in absolute reflectance in the red and 25% in the IR (750 nm). The mean value of red reflectance for the wet soils was computed to be 20.5% $\pm$ 13.1%. In the IR the mean reflectance was 23.8% $\pm$ 13.8%.

In every case, the wet soil was found to have a lower reflectance than the dry soil in all spectral regions. Furthermore, the absolute decrease was generally less in low reflecting spectral regions than in high reflecting regions. This situation suggests that the percent relative change might be similar in two spectral regions, and that a ratio of reflectance in two spectral band signals might be an effective normalizer of soil moisture.

Accordingly, ratios were computed for all of the wet soils. The 750/650 ratio had a mean value of 1.20 and a standard deviation of 0.11. The variability in the ratio was even smaller within the three soil "classes" identified by Condit.

The relative variability of reflectance was calculated for the individual bands and the IR/red ratio by dividing the standard deviation by the mean value. These results are summarized in Table I-j.

TABLE I-j. VARIABILITY IN SOIL REFLECTANCE FOR WET SOILS AND FOR DRY SOILS

Red		IR		IR/Red	
Dry	Wet	Dry	Wet	Dry	Wet
.48	.65	.42	.58	.10	.09

It can be seen that the variability is considerably less for the ratio, both for wet and dry soils.

If the soils are stratified into the three general "classes" of soils of Condit, the variability can be reduced even further. For example, for the most common general soil class (representing 16 different soils), the ratio of the standard deviation divided by the mean is presented in Table I-k.

TABLE I-k. VARIABILITY IN SOIL REFLECTANCE FOR A PARTICULAR GENERAL SOIL CLASS (16 soils).

Red		IR		IR/Red	
Dry	Wet	Dry	Wet	Dry	Wet
.35	.51	.33	.49	.05	.05

The mean value of the IR/Red ratio for the soils in this class is 1.11 for dry soil and 1.12 for wet soil, less than a 1% difference.

The behavior of reflectance was also investigated for variability of soil moisture at various levels between "dry" and "wet", using data of Bowers and Hanks[25]. The red and IR reflectance both decrease continuously as soil moisture increases. The IR/red reflectance ratio, on the other hand, remains virtually constant and equal to the dry and wet values.

The reflectance values of all soils in both the wet and dry state were subsequently analyzed together. The relative variability was again calculated by dividing the standard deviation by the mean. The results are presented in Table I-1. As can be seen, the variability is again much smaller for the ratio than for either spectral region individually.

TABLE I-1. VARIABILITY IN SOIL REFLECTANCE FOR ALL SOILS IN BOTH THE WET AND DRY STATE

RED			IR			IR/RED		
$\overline{X}$	σ	$\sigma/\overline{X}$	X	σ	$\sigma/\overline{X}$	X	σ	$\sigma/\overline{X}$
26.90	15.85	.59	30.99	16.59	.54	1.19	.11	.09

Apparently, then, the 750/650 ratio (and perhaps other ratios) is a very effective normalizer of both variability in soil type and moisture content, simultaneously. If the soils are grouped into classes as Condit did, the ratio is an almost perfect normalizer of these phenomena.

Another question that needs to be addressed, however, is whether this ratio is useful for differentiating between different species of crops or different crop conditions. That question can generally be answered in the affirmative.

At any one time crops might be different from each other in terms of crop structure (morphology), amount of vegetative cover and/or projected

[25] Bowers, S.A., and R.J. Hanks. 1965. "Reflection of Radiant Energy From Soils." Soil Science, Vol. 100 #2.

leaf area index. J. Colwell[16] and others have found that the 750/650 reflectance ratio is quite sensitive to changes in phenomena such as these. For example, two plant canopies with the same amount of accumulated material (biomass), but different canopy structure were found to be markedly different in their 750/650 reflectance ratios. And the 750/650 reflectance ratio was found to be an excellent indicator of percent cover and projected leaf area index.

However, the 750/650 ratio is not a panacea for data normalization or crop species/yield determination. For example, this ratio is <u>not</u> a perfect normalizer of effects of solar zenith angle (which changes during the growing season) or amount of dead or chlorotic material which is present in the plant canopy. In addition, there may be soils with different characteristics than those represented here for which ratioing is not as useful.

These problems need to be more thoroughly investigated. Only after a thorough analysis of these and other factors (such as angle of view) can one determine what is gained and what is lost by any data collection or processing procedure. Only after such a thorough analysis is it possible to know how to interpret the data under varying conditions. Clearly, there are so many variable factors involved that the problem must be approached initially by analytical modeling. Once this is done, a realistic and effective empirical investigation plan can be constructed for validating the results of modeling.

---

[16] Colwell, J. 1973. "Bidirectional Spectral Reflectance of Grass Canopies for Determination of Above Ground Standing Biomass." Ph.D. Dissertation, University of Michigan, Ann Arbor, Michigan.

APPENDIX II
YIELD TRANSFORMATION

There are a number of ways the relationship between moles fixed CO_2/m^2 and bushels/acre of grain yield can be approximately determined. The following is a description of one such method.

The basic reaction involved in photosynthesis is:

$$6CO_2 + 6H_2O \rightarrow C_6H_{12}O_6 + 6O_2$$

If we make the simplifying assumption that wheat grain is basically $C_6H_{12}O_6$ or reasonable equivalent then we can assume that it takes 6 moles of CO_2 to make a mole of grain yield ($C_6H_{12}O_6$).

A bushel of wheat weighs approximately 60 lbs (Safir, personal communication; Jebe, personal communication), or .453 x 60 = 27.18 kg. Since a mole of $C_6H_{12}O_6$ weighs 180 gms, a bushel is

$$27.18 \text{ kg/bushel} / .18 \text{ kg/mole} = 151 \text{ moles fixed } C_6H_{12}O_6\text{/bushel}$$
$$= 906 \text{ moles fixed } CO_2\text{/bushel}$$

Since one acre is 4047 square meters, one bushel of wheat/acre =

$$\frac{906 \text{ moles } CO_2}{4047 \text{ m}^2} = \frac{.224 \text{ moles } CO_2}{\text{m}^2}$$

Therefore, 50 bushels/acre = 11.2 moles CO_2/m^2.

APPENDIX III

RULES FOR ASSIGNING TOTAL AREA TO COMPONENT PROJECTED AREAS

I) Before Heading Geometry Rules

The ratio of leaf area to stalk area is approximated from published data as a function of days after first spring growth.

$$A(leaf)/A(stalk) = 4\ (NDY-85)/70 + 4.$$

Thus

$$A(stalk) = A(NDY)/(1 + A(leaf)/A(stalk).$$

Hence

$$A(leaf) = A(NDY) - A(stalk)$$

Orientation of these total areas are then as follows:

$$H(leaf) + 0 = A(NDY) * ASP$$

and since

$$V(leaf) + V(stalk) = (1-ASP) * A(NDY)$$

then

$$V(leaf) = (1-ASP) * A(NDY) - A(stalk)$$

where

$$A(stalk) = V(stalk)$$

$$X_1 = -.5,\ X_2 = -1.0, \text{ for all times before heading.}$$

"A" represents the total projected in the canopy (both layers for the indicated component).

"NDY" is the day of the year.

"ASP" is the ratio of horizontal projected area to the total projected area.

"X"$_{1,2}$ is the distance from the top of the canopy through the first and second layer of the canopy of unit thickness.

"H","V" are the horizontal and vertical projected leaf area indices, respectively.

II) SLOUGH OFF AND BEFORE STALK NECROSIS RULES

Determine A(peak).

Then A(necrotic) = 1/2 (A(peak) - 1/8 A(peak)) by shrivel factor, and because A(stalk) is 1/8 A(NDY) at time of heading.

H_2(necrotic leaf) = .1 * A(necrotic).

V_2(necrotic leaf) = .9 * A(necrotic).

$$X_1 = -\left(1 - \frac{A(peak) - A(NDY)}{A(peak) - 1/2\ A(peak)}.\right)$$

where

A(stalk) = 1/8 A(peak) and remains fixed.

$-1.0 < X_1 < 0.$

$X_2 = -1.00.$

H_2 and V_2 are both layer 2 necrotic class.

H_1(green healthy) = A(peak) * ASP.

V_1(green healthy) = A(peak) * (1 - ASP) - 1/8 A(peak).

III) STALK NECROSIS RULES

Stalk necrosis begins when $A(NDY) \leq 1/8\ A(peak)$

$1/8\ A(peak) = V(\text{stalk healthy}) + V(\text{stalk necrotic})$.

Since all of A(NDY) refers to V(stalk healthy) then stalk values are changed so that

$V_{1,2}(\text{stalk healthy}) = A(NDY)$

$V_{1,2}(\text{stalk necrotic}) = 1/8\ A(peak) - A(NDY)$

$X_1 = -.001$

$X_2 = -1.000$

All other values are used as in II.

APPENDIX IV
DETAILED PERFORMANCE OF THE GROWTH MODEL

Hourly values of a number of important parameters calculated by the Growth Model were printed out for selected days in an attempt to assess the performance of the model. The following discussion concentrates on calculated values of transpiration and net photosynthesis.

Transpiration

The following discussion presents material concerning the hourly transpiration values for a number of days presented in Figure IV-a. The number 12 on the abscissa represents the twelfth hour of the day. Day 90 was a sunny day, the P.L.A.I. was .38, and the soil moisture was not an inhibiting factor. Note that the transpiration value is zero at hours 5 and 19 due to stomatal closure caused by inadequate illumination. The discontinuity in the curve is somewhat of an artifact caused by values being computed only once an hour. Day 110 was partly cloudy (half sunny, half cloudy). The P.L.A.I. was .92, and there was adequate soil moisture. The transpiration value is higher at all corresponding hours of the day due to a greater P.L.A.I. and a higher temperature which caused a greater air moisture potential. Day 140 was a cloudy day, the P.L.A.I. was 2.92, and the soil moisture was adequate. Note that with the longer daylength of day 140, the stomates remain open on hours 5 and 19. Even though the day was cloudy, the transpiration value was greater than on previous days due to the greater P.L.A.I. and the greater temperature of each corresponding hour. Note also the lag in the peak transpiration value until hour 14, which is largely due to the daily lag in temperature which was incorporated into the model.

Net Photosynthesis

Hourly values of net photosynthesis were computed for the same days as transpiration. The results are graphed in Figure IV-6. Note that the net photosynthesis curves are not entirely different from the transpiration

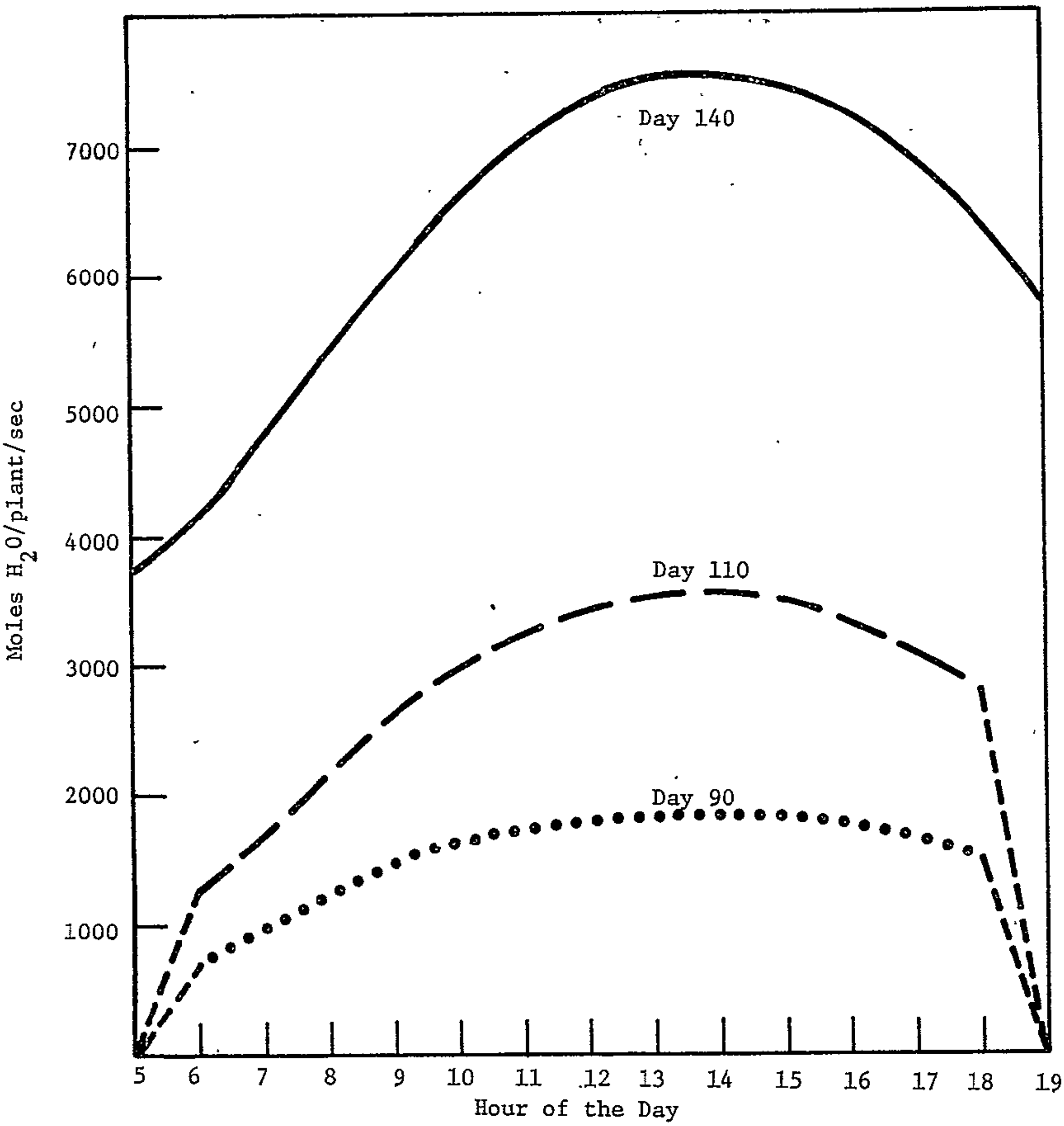

Figure IV-a. Hourly Values of Transpiration For Three Days in the Growing Season. (The Abrupt Fall-Off at Hours 6 + 18 for Days 90 and 110 Indicates that the Value Goes To Zero During The Hour).

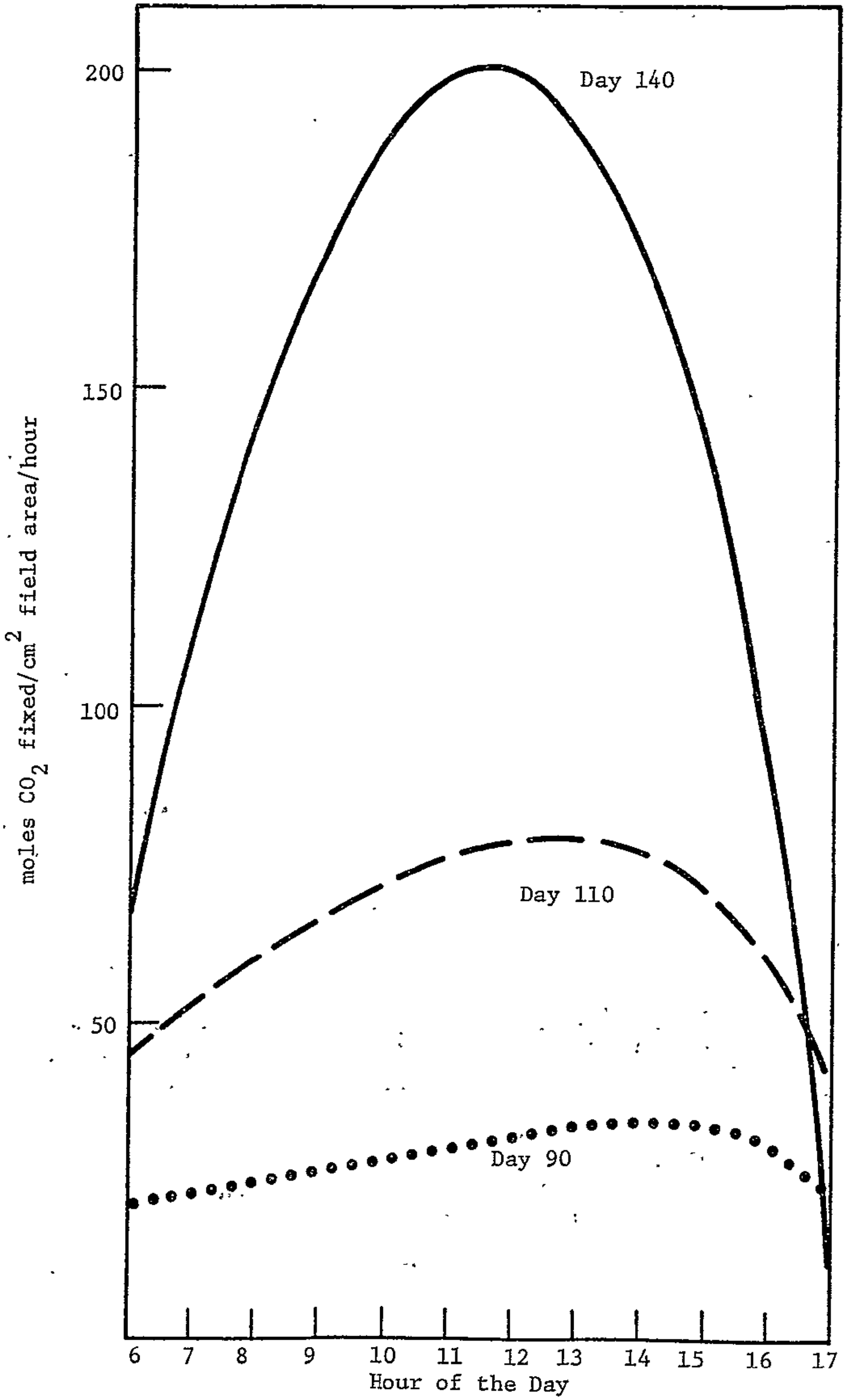

Figure IV-b. Hourly Vaules of Net Photosynthesis For Three Days in the Growing Season

curves. The similarity in the respective curves is due to the fact that stomatal resistance is one of the main things controlling both transpiration and photosynthesis.

However, there are significant differences in the transpiration and net photosynthesis curves. Gross photosynthesis is very sensitive to the level of illumination. Gross photosynthesis of wheat is quite sensitive to temperature at low values of temperature (<15°C) and rather insensitive at high values of temperature, whereas the response of respiration is exactly opposite with respect to temperature. Net photosynthesis is the difference between gross photosynthesis and respiration.

Only positive values of net photosynthesis are graphed in Figure IV-6. Positive net photosynthesis begins at the same hour of the morning as transpiration for days 90 and 110. This is probably because the stomates are open and there is sufficient light for photosynthesis, but not such high temperatures that respiration is significant compared to gross photosynthesis. Positive net photosynthesis for these two days ceases before the corresponding hour for transpiration, however, probably because of the temperature lag causing respiration to be a more significant factor late in the day. This same factor probably also accounts for the premature cutoff of net photosynthesis for day 110 as compared to transpiration for the same day.

The shift in the peak value of net photosynthesis towards earlier in the day from day 90 to day 140 probably represents the greater relative response of respiration to the built-in temperature lag at increasingly high values of temperature, and the smaller relative response of gross photosynthesis.

GLOSSARY

Growth Model: A model which predicts the development of a vegetation canopy, especially the amount of photosynthetic material produced (see Section 2.1).

Yield Model: A model which predicts yield, generally using a regression equation of meteorological variables (see Section 2.1).

Biological Leaf Area Index: the total one-sided area of leaves per unit area of ground (see Section 3.1)

Projected Leaf Area Index: orthogonal projections of vegetative material simulating idealized biological components (See Figure 2).

Percent Vegetation Cover: the percent of ground area obscured by vegetation when looking straight down at the canopy (See Appendix I).

REFERENCES

1. Suits, G.H., 1972, "The Calculation of the Directional Reflectance of a Vegetative Canopy", Remote Sensing of Environment, V. 2, pp. 117-125.

2. Thompson, L.M., 1969, "Weather and Technology in the Production of Wheat in the United States", Journal of Soil and Water Conservation, V 24 #6, Proceedings of the IBP/PP Technical Meeting, Trebon, Published by Centre for Agricultural Publishing and Documentation, Wageningen, The Netherlands.

3. Baier, W., 1973, "Crop-Weather Analysis Model: Review and Model Development", Journal of Applied Meteorology, V. 12 #6.

4. Chartier, Ph. 1970. "A Model of CO_2 Assimilation in the Leaf", In Prediction and Measurement of Photosynthetic Productivity. Proceedings of the IBP/PP Technical Meeting. Trebon. Published by Centre for Agricultural Publishing and Documentation, Wageningen, The Netherlands.

5. Lommen, P.W., C.R. Schwintzer, C.S. Yocum, and D.M. Gates, 1971, "A Model Describing Photosynthesis in Terms of Gas Diffusion and Enzyme Kinetics", Planta (Berl.) 98, 195-220.

6. Ross, J., 1970, "Mathematical Models of Photosynthesis in a Plant Stand", In Prediction and Measurement of Photosynthetic Productivity, Proceedings of the IBP/PP Technical Meeting, Trebon, Published by Centre for Agricultural Publishing and Documentation, Wageningen, The Netherlands.

7. Van Keulen, H., and W. Louwerse, 1973, "Simulation Models for Plant Production", W.M.O. Symposium on Agrometeorology of the Wheat Crop, Braunschweig, Germany.

8. Tooming, H., 1970, "Mathematical Description of Net Photosynthesis and Adaptation Processing in the Photosynthetic Appartus of Plant Communities", In Prediction and Measurement of Photosynthetic Productivity.

9. Monsi, M., 1968, "Mathematical Models of Plant Communities", Functioning of Terrestrial Ecosystems at the Primary Production Level, Proc. Copenhagen Symposium, UNESCO pp. 131-144.

10. Duncan, W.G., Loumis, R.S., Williams, W.A., and R. Hanau, 1967, "A Model for Simulating Photosynthesis in Plant Communities", Hilgardia: 38, pp. 181-205.

11. Haun, J.R., 1973, "Evaluation of Wheat Development Relative to Environment From Quantitative Morphological Data", Symposium on Agrometeorology of the Wheat Crop, World Meteorological Organization. Braunschweig, Germany.

REFERENCES (continued)

12. de Wit, C.T., R. Brouwer, and F.W.T. Penning de Vries, 1971, "A Dynamic Model of Plant Growth", in Potential Crop Production, Edited by P.F. Waring and J.P. Cooper, Heinemann Education Book Ltd., London.

13. Lupton, F.G.H., 1972, "Further Experiments on Photosynthesis and Translocation in Wheat", Ann. Appl. Biol. 71:69-79.

14. Miles, G.E., R.J. Bula, D.A. Holt, M.M. Shcreiber, and R.M. Peart, 1973, "Simulation of Alfalfa Growth", American Society of Agricultural Engineers, Paper No. 73-4547, St.Joseph, Michigan,

15. Waggoner, P.E., 1970, "Consultation on How Models are Made, How They Are Tested, and What They Tell Us of Experiments to be Done", In Prediction and Measurement of Photosynthetic Productivity. Proceedings of the IBP/PP Technical Meeting, Trebon, Published by Centre for Agricultural Publishing and Documentation, Wageningen, The Netherlands,

16. Colwell, J., 1973, "Bidirectional Spectral Reflectance of Grass Canopies for Determination of Above Ground Standing Biomass", PhD Dissertation University of Michigan, Ann Arbor, Michigan.

17. Welbank, P.J., S.A.W. French, and K.J. Witts, 1966, "Dependence of Yields of Wheat Varieties on Their Leaf Area Durations", Annals of Botany, N.S. Vol. 30, No. 118.

18. Stoy, V., 1965, "Photosynthesis, Respiration, and Carbohydrate Accumulation in Spring Wheat in Relation to Yield", Physiologia Plantarum Supplementum, IV.

19. Strebeyko, P., M. Wislocka, and T. Krzywacka, 1963, "Dynamics of Growth and Development in Spring Wheat", Physiologia Plantarum, Vol. 16.

20. Safir, G.R., G.H. Suits, and M.V. Wiese, 1972, "Application of a Directional Reflectance Model to Wheat Canopies Under Stress", Presented at International Conference on Remote Sensing in Arid Lands, Tuscon, Arizona.

21. ITEK, 1965, Photographic Considerations for Aerospace, p. 15.

22. Suits, G.H., and G.R. Safir, 1972, "Verification of a Reflectance Model for Mature Corn with Applications to Corn Blight Detection", Remote Sensing of Environment, V. 2, pp 183-192.

REFERENCES (continued)

23. Condit, H.R., 1970, "The Spectral Reflectance of American Soils", Photogrammetric Engineering, V. 36 #9, pp 955-966.

24. Nazare, C. 1973, "An Analysis of Laboratory Hemispherical Reflectance Spectra of Selected Rocks in the Wavelength Range 0.35 to 3.50 Micrometer", M.S. Thesis University of Michigan, Ann Arbor, Michigan.

25. Bowers, S.A., and R.J. Hanks, 1965, "Reflection of Radiant Energy from Soils", Soil Science, Vol. 100 #2.

Technical and Final Report Distribution List

NASA Contract NAS9-14123

Tasks II thru X

NAME	NUMBER OF COPIES
NASA/Johnson Space Center Earth Observations Division Houston, Texas 77058	
ATTN: Mr. Robert MacDonald/TF	(1)
ATTN: Mr. B. Erb/TF2	(1)
ATTN: Dr. F. Hall/TF2	(1)
ATTN: Mr. J. Murphy/TF2	(1)
ATTN: Dr. A. Potter/TF3	(8)
ATTN: Mr. J. Dragg/TF4	(1)
ATTN: Earth Resources Data Facility/TF12	(8)
NASA/Johnson Space Center Earth Resources Program Office Office of the Program Manager Houston, Texas 77058	
ATTN: Mr. Clifford E. Charlesworth/HA	(1)
ATTN: Mr. William E. Rice/HA	(1)
NASA/Johnson Space Center Earth Resources Program Office Program Analysis & Planning Office Houston, Texas 77058	
ATTN: Dr. O. Glenn Smith/HD	(1)
NASA/Johnson Space Center Earth Resources Program Office Systems Analysis and Integration Office Houston, Texas 77058	
ATTN: Mr. Richard A. Moke/HC	(1)
ATTN: Mr. M. Jay Harnage, Jr./HC	(1)
NASA/Johnson Space Center Technical Library Branch Houston, Texas 77058	
ATTN: Ms. Retha Shirkey/JM6	(4)

NAME	NUMBER OF COPIES
NASA/Johnson Space Center Management Services Division Houston, Texas 77058 ATTN: Mr. John T. Wheeler/AT3	(1)
NASA/Johnson Space Center Technical Support Procurement Houston, Texas 77058 ATTN: Mr. J. Haptonstall/BB63	(1)
Earth Resources Laboratory, GS Mississippi Test Facility Bay St. Louis, Mississippi 39520 ATTN: Mr. D. W. Mooneyhan	(1)
EROS Data Center U.S. Department of Interior Sioux Falls, South Dakota 57198 ATTN: Mr. G. Thorley	(1)
Department of Mathematics Texas A&M University College Station, Texas 77843 ATTN: Dr. Larry Guseman	(1)
NASA/Johnson Space Center Computation & Flight Support Houston, Texas 77058 ATTN: Mr. Eugene Davis/FA	(1)
U.S. Department of Agriculture Agricultural Research Service Washington, D.C. 20242 ATTN: Dr. Robert Miller	(1)
U.S. Department of Agriculture Soil & Water Conservation Research Division P.O. Box 267 Weslaco, Texas 78596 ATTN: Dr. Craig Wiegand	(1)

NAME	NUMBER OF COPIES
U.S. Department of Interior Geology Survey Washington, D.C. 20244 ATTN: Dr. James R. Anderson	(1)
Director, Remote Sensing Institute South Dakota State University Agriculture Engineering Building Brookings, South Dakota 57006 ATTN: Mr. Victor I. Myers	(1)
U.S. Department of Interior Fish & Wildlife Service Bureau of Sport Fisheries & Wildlife Northern Prairie Wildlife Research Center Jamestown, North Dakota 58401 ATTN: Mr. Harvey K. Nelson	(1)
U.S. Department of Agriculture Forest Service 240 W. Prospect Street Fort Collins, Colorado 80521 ATTN: Dr. Richard Driscoll	(1)
U.S. Department of Interior Geological Survey Water Resources Division 500 Zack Street Tampa, Florida 33602 ATTN: Mr. A.E. Coker	(1)
U.S. Department of Interior Director, EROS Program Washington, DC 20244 ATTN: Mr. J. M. Denoyer	(1)
U.S. Department of Interior Geological Survey GSA Building, Room 5213 Washington, DC 20242 ATTN: Mr. W.A. Fischer	(1)

NAME	NUMBER OF COPIES
NASA Wallops Wallops Station, Virginia 23337	
ATTN: Mr. James Bettle	(1)
Purdue University Purdue Industrial Research Park 1200 Potter Drive West Lafayette, Indiana 47906	
ATTN: Dr. David Landgrebe	(1)
ATTN: Dr. Philip Swain	(1)
ATTN: Mr. Terry Phillips	(1)
U.S. Department of Interior EROS Office Washington, DC 20242	
ATTN: Dr. Raymond W. Fary	(1)
U.S. Department of Interior Geological Survey 801 19th Street, N.W. Washington, DC 20242	
ATTN: Mr. Charles Withington	(1)
U.S. Department of Interior Geological Survey 801 19th Street, N.W. Washington, DC 20242	
ATTN: Mr. M. Deutsch	(1)
U.S. Geological Survey 801 19th Street, N.W., Room 1030 Washington, DC 20242	
ATTN: Dr. Jules D. Friedman	(1)
U.S. Department of Interior Geological Survey Federal Center Denver, Colorado 80225	
ATTN: Dr. Harry W. Smedes	(1)

NAME	NUMBER OF COPIES
U.S. Department of Interior Geological Survey Water Resources Division 901 S. Miami Ave. Miami, Florida 33130 ATTN: Mr. Aaron L. Higer	(1)
University of California School of Forestry Berkeley, California 94720 ATTN: Dr. Robert Colwell	(1)
School of Agriculture Range Management Oregon State University Corvallis, Oregon 97331 ATTN: Dr. Charles E. Poulton	(1)
U.S. Department of Interior EROS Office Washington, DC 20242 ATTN: Mr. William Hemphill	(1)
Chief of Technical Support Western Environmental Research Laboratories Environmental Protection Agency P.O. Box 15027 Las Vegas, Nevada 89114 ATTN: Mr. Leslie Dunn	(1)
NASA/Langley Research Mail Stop 470 Hampton, Virginia 23365 ATTN: Mr. William Howle	(1)
U.S. Geological Survey Branch of Regional Geophysics Denver Federal Center, Building 25 Denver, Colorado 80225 ATTN: Mr. Kenneth Watson	(1)

NAME	NUMBER OF COPIES
NAVOCEANO, Code 7001 Naval Research Laboratory Washington, DC 20390 ATTN: Mr. J. W. Sherman, III	(1)
U.S. Department of Agriculture Administrator Agricultural Stabilization and Conservation Service Washington, DC ATTN: Mr. Kenneth Frick	(1)
Pacific Southwest Forest & Range Experiment Station U.S. Forest Service P. O. Box 245 Berkeley, CA 94701 ATTN: Mr. R. C. Heller	(1)
United States Department of Agriculture/Forestry Service Division of Forest Economics and Marketing Resources 1200 Independence Avenue Washington, D.C. 20250 ATTN: Dr. P. Weber	(1)
University of Texas at Dallas Box 688 Richardson, Texas 75080 ATTN: Dr. Patrick L. Odell	(1)
Department of Mathematics University of Houston Houston, Texas 77004 ATTN: Dr. Henry Decell	(1)
Institute for Computer Services and Applications Rice University Houston, Texas 77001 ATTN: Dr. M. Stuart Lynn	(1)

NAME	NUMBER OF COPIES
U.S. National Park Service Western Regional Office 450 Golden Gate Avenue San Francisco, California 94102 ATTN: Mr. M. Kolipinski	(1)
U.S. Department of Agriculture Statistical Reporting Service Washington, DC 20250 ATTN: D. H. VonSteen/R. Allen	(2)
U.S. Department of Agriculture Statistical Reporting Service Washington, DC 20250 ATTN: Mr. H. L. Trelogan, Administrator	(1)
Department of Watershed Sciences Colorado State University Fort Collins, Colorado 80521 ATTEN: Dr. James A. Smith	(1)
Lockheed Electronics Co. 16811 El Camino Real Houston, Texas 77058 ATTN: Mr. R. Tøkerud	(1)
TRW System Group Space Park Drive Houston, Texas 77058 ATTN: Dr. David Detchmendy	(1)
IBM Corporation 1322 Space Park Drive Houston, Texas 77058 ATTN: Dr. D. Ingram	(1)
S&D - DIR Marshall Space Flight Center Huntsville, Alabama 35812 ATTN: Mr. Cecil Messer	(1)

NAME	NUMBER OF COPIES
Code 168-427 Jet Propulsion Laboratory 4800 Oak Grove Drive Pasadena, California 91103	
ATTN: Mr. Fred Billingsley	(1)
NASA Headquarters Washington, DC 20546	
ATTN: Mr. W. Stoney/ER	(1)
ATTN: Mr. Leonard Jaffe/ER	(1)
ATTN: Mr. M. Molloy/ERR	(1)
ATTN: Mr. James R. Morrison	(1)
Ames Research Center National Aeronautics and Space Administration Moffett Field, California 94035	
ATTN: Dr. D. M. Deerwester	(1)
Goddard Space Flight Center National Aeronautics and Space Administration Greenbelt, Maryland 20771	
ATTN: Mr. W. Nordberg, 620	(1)
ATTN: Mr. W. Alford, 563	(1)
Lewis Research Center National Aeronautics and Space Administration 21000 Brookpark Road Cleveland, Ohio 44135	
ATTN: Dr. Herman Mark	(1)
John F. Kennedy Space Center National Aeronautics and Space Administration Kennedy Space Center, Florida 32899	
ATTN: Mr. S. Claybourne/FP	(1)
NASA/Langley Mail Stop 214 Hampton, Virginia 23665	
ATTN: Mr. James L. Raper	(1)

NAME	NUMBER OF COPIES
Texas A&M University Institute of Statistics College Station, TX 77843 ATTN: Dr. H. O. Hartley	(1)
Texas Tech University Department of Mathematics P. O. Box 4319 Lubbock, TX 79404 ATTN: Dr. T. Boullion	(1)
Mr. James D. Nichols Space Sciences Laboratory, Rm. 260 University of California Berkeley, CA 94720	(1)
EXXON Production Research Co. P. O. Box 2189 Houston, TX 77001 ATTN: Mr. J. O. Bennett	(1)